The Plastic and Adaptive Evolutionary Potential of Nonstructural Carbohydrates in a Temperate Tree Species

HARVARD UNIVERSITY
Graduate School of Arts and Sciences

DISSERTATION ACCEPTANCE CERTIFICATE

The undersigned, appointed by the

Department of Organismic and Evolutionary Biology

have examined a dissertation entitled

"The Plastic and Adaptive Evolutionary Potential of Nonstructural Carbohydrates in a Temperate Tree Species"

presented by

Meghan Blumstein

candidate for the degree of Doctor of Philosophy and hereby

certify that it is worthy of acceptance.

Signature N. Michele Holbrook
N. Michele Holbrook (Aug 7, 2020 15:10 EDT)

Typed name: Professor Noel Michele Holbrook

Signature Robin Hopkins
Robin Hopkins (Aug 6, 2020 14:42 EDT)

Typed name: Professor Robin Hopkins

Signature Elena Kramer

Typed name: Professor Elena Kramer

Signature Jonathan Thompson
Jonathan Thompson (Aug 6, 2020 11:51 EDT)

Typed name: Jonathan Thompson

Date: August 6, 2020

The Plastic and Adaptive Evolutionary Potential of Nonstructural Carbohydrates in a Temperate Tree Species

A dissertation presented by

Meghan Blumstein

to

The Department of Organismic and Evolutionary Biology

in partial fulfillment of the requirements
for the degree of

Doctor of Philosophy

in the subject of

Biology

Harvard University
Cambridge, Massachusetts
August 2020

Dissertation Advisor: Dr. Noel M. Holbrook Meghan Blumstein

The Plastic and Adaptive Evolutionary Potential of Nonstructural Carbohydrates in a Temperate Tree Species

ABSTRACT

The ability to undergo plastic and evolutionary change in adaptive traits is key for plant survival under future climate change. Both processes require genetic variation in adaptive traits within populations. Thus, for my dissertation I measured genetic variation in nonstructural carbohydrates (NSC) storage concentrations, a critical trait that provides resilience to tree species during times of stress, within two common gardens. Both gardens had the same 1,100 genotypes, sourced from 19 different populations, and clonally replicated 3x at each site, as well as full genomic sequences for all genotypes. Common gardens are ideal as they control for differences in environment, allowing researchers to parse phenotypic differences due to genetics (ie. genetic variation). I sampled the branches, stems, and roots of black cottonwood (*Populus trichocarpa*) trees in two different Department of Energy (DOE) common gardens in January 2017.

In Chapter 1, I demonstrate the presence of locally adapted, genetic variation in NSC storage in the stems and roots of black cottonwood trees, indicating the potential for range-wide adaptive evolution. Using a novel model of allele frequency distribution and climate, I predict that northern populations will be limited in their ability to adapt to future climates by a lack of genetic variation, while southern populations have high genetic diversity, but are at risk of local extinction due to more intense selective pressures.

In Chapter 2, I compare genetic variation in NSC stores to genetic variation in other traits to look for locally adapted tradeoffs. I discover a tradeoff between NSC storage and diameter growth/fungal pathogen resistance when traits are relativized for differences in carbon supply. This tradeoff is not current locally adapted, but populations exhibit high variation in the degree to which plants store vs. grow/defend, indicating an evolutionary potential.

Finally, in Chapter 3 I explore genetic and plastic variation in branch total NSC concentrations and the proportion of NSC that resides in soluble sugars (ie. affect cell osmotic balance) and insoluble starch. I find genetic and plastic variation in both traits. Moving from the coastal (Clatskanie) to continental (Corvallis) garden, there was a 50% decrease in the average amount NSC stored as starch. There was no difference in the total amount of NSC concentrations between the two gardens. However, trees in Clatskanie grew much faster and were larger than trees in Corvallis, despite maintaining the same concentration of NSC in their tissues. Our findings suggest that a NSC storage – growth tradeoff may also be plastic.

Contents

Acknowledgments

This work would not be possible without the team of people who have supported and mentored me along the way. First, I am forever grateful to Jonathan Thompson for taking a chance and hiring me as his research assistant, setting me off on my path as a scientist, and for his continued support even after I left his lab. I would like to thank Andrew Richardson for supporting early phases of this project and connecting me with David Weston, who facilitated my use of the common gardens and was a wonderful and welcoming mentor for the months I spent was at Oak Ridge National Lab. I also would like to thank Elena Kramer for advocating for me as a graduate student and connecting me with the resources I needed to become an independent scientist. Finally, I would like to exuberantly thank Missy Holbrook and Robin Hopkins for serving as my mentors and coaches during my graduate tenure. Missy, I will forever be grateful for you taking me on in your lab and the incredible female-empowered environment you created therein. Robin, despite our disparate fields, you never stopped fighting for me as a scientist. You took the time out of your schedule to meet with me regularly, pick me up when I failed, and read *every* draft of my writing. I hope to be able to one day pass on your kindness to the next generation of scientists.

Beyond my mentors, I would like to thank my wonderful support system of family and friends in Cambridge and beyond. In particular, many thanks to my partner Connor, not only for his constant support, but his assistance in both of my field campaigns and willingness to dig roots in 100^{O}F head or 18^{O}F cold. Finally, my friend and colleague Morgan Furze, who's shared passion for NSCs and frozen yogurt made the experience of working long days in lab much more enjoyable.

All material herein is based upon work supported by the U.S. Department of Energy, Office of Science, Office of Workforce Development for Teachers and Scientists, Office of Science Graduate Student Research (SCGSR) program, by the National Science Foundation Graduate Research Fellowship under Grant No. DGE1745303, and the Explorer's club. The SCGSR program is administered by the Oak Ridge Institute for Science and Education (ORISE) for the DOE. ORISE is managed by ORAU under contract number DE-SC0014664.

Introduction

Motivation

Forests cover 30% of the world's land surface[1]and are a net sink of 1.1 +- 0.8 Pg C/year, which accounts for about 40% of our annual fossil fuel emissions[2]. However, climate change is causing large-scale alterations to forest communities [3,4]. Even under conservative scenarios, future climate changes are likely to include further increases in mean temperature (0.3 – 4.8^{0}C globally) over the 0.85^{0}C it has already warmed during the past century, with significant increases in frequency and severity of extreme droughts, temperatures, and storms[5]. These changes are happening at a very rapid rate and may outstrip forests' ability to adapt. Thus, climate changes has the potential to produce major shifts in vegetation distributions at unprecedented rates in the coming decades[6-8]. In order to understand the fate of vegetation, we must first understand what mechanisms trees can employ to persist on the landscape for decades to centuries. By understanding the genetic and environmental controls on these adaptive traits, their drivers, and constraints, we will be able to secure a better picture of the rate and direction of change in future forest communities.

Nonstructural Carbohydrates

The storage of nonstructural carbohydrates is a trait that has been hypothesized to provide trees with long-term resilience[9-12]. Nonstructural carbohydrates are the sugars, primarily glucose, fructose, and sucrose, and starch that are produced by trees during photosynthesis that are not immediately used for growth or reproduction, but rather are stored in the ray and parenchyma cells of a tree's woody tissues (branch, stem, roots) [13,14]. Like an animal's fat stores, these labile sugars and starch represent the total energetic stores of the tree and serve as a vital buffer for plants in stressful times when demand (growth, protection, metabolism, etc.) exceeds current photosynthetic supply, such as during the dormant season or in response to environmental stress/disturbance[15].

It is important to note that sugar allocation to storage is not constant, but follows distinct patterns on several different time scales, from small diurnal fluxes between daytime accumulation and nighttime use, to annual fluxes over the course of the growing and dormant season[9,16-19]. In general, woody perennial plants growing in seasonal environments draw down their sugar stores when growth is most rapid (mid-summer) and reach a peak in sugars during the dormant season; while starch holds the opposite pattern (Figure 1). These trends hold true for carbon stores in temperate, deciduous tree species, both diffuse and ring-porous[16,20]. Nonstructural carbohydrates are also moved and mixed within tissues. Across the outer segments of stem tissue, for example, there is a high degree of radial mixing of stores[21] and stores have also been shown to decline radially with increasing distance from the cambium, which has been linked to parenchyma cell death and heartwood formation[14].

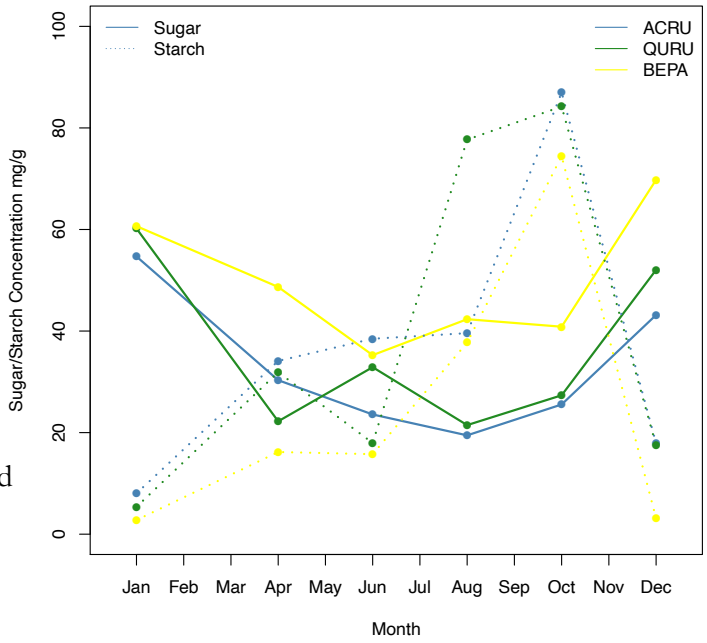

Figure 1. Branchwood sugar and starch concentrations from Harvard Forest in 2015. ACRU = Acer Rubrum, QURU = Quercus Rubrum, and BEPA = Betula Papirifera. Adapted from Furze et al. 2019.

Study Species

My study will focus on *Populus trichocarpa* (Black Cottonwood), a wide-ranging, fast growing species that has become the model for genomic studies in woody species [22]. *P. trichocarpa* is an ideal species for this study as it inhabits a wide-array of environments and exhibits a diversity of phenotypes across its range[23-26]. *P. trichocarpa* can be found from isolated populations in the Aleutian Islands down to a few refugia in northern Baja and into central Canada, Montana, and Idaho[27](Figure 2). Across this expanse, black cottonwood experiences a large range in climatic conditions, with annual precipitation ranging from 250 mm to 3,050 mm, minimum temperatures ranging from -47°C - 0°C, and maximum temperature ranging from 16°C - 47°C[27]. These large clines in temperature and precipitation will allow me to quantify how one species might survive under a variety of extreme conditions.

P. trichocarpa can both vegetative and sexually reproduce. It is a dioecious species, having separate male and female catkins, but also resprouts readily via stump or root sprouting following disturbance. More uniquely, *P. trichocarpa* may abscise small shoots from their branches, complete with leaves, which can establish where they fall or be dispersed via water transport [27]. Its fast growth and ease of reproduction also make it an ideal species to propagate.

Finally, *P. trichocarpa* is ideal as it has become the models species for forest-tree genome studies since its genome was first sequenced in 2006[22,28]. *Populus* has a relatively modest genome size in comparison to other flowering plant species at around 417 Mega base pairs (Mbp) long, but still lengthy in comparison to other organisms (*Arabidopsis* ~ 135 Mbp)[22]. It is a diploid species with a haploid number of 19 chromosomes, with no definitive sex chromosomes [29]. So far, 41,377 protein-coding gene loci have been identified in the nuclear genome (Tuskan et al. 2006; EnsemblPlants 2015). Sequencing in 2006 revealed widespread patterns of linkage disequilibrium (LD) and population structure and previous and subsequent studies have demonstrated the prevalence of local adaptation[eg28] (ex. Evans et al. 2014).

1

A new perspective on ecological prediction reveals limits to climate adaptation in a temperate tree species

Reprinted from:

Blumstein, MJ, Richardson, AD, Weston, D, Zhang, J, Muchero, W, Hopkins, R. 2020. A new perspective on ecological prediction reveals limits to climate adaptation in a temperate tree species. *Current Biology* 30:1-7.

Article and supplement available at https://doi.org/10.1016/j.cub.2020.02.001

Article

Current Biology

A New Perspective on Ecological Prediction Reveals Limits to Climate Adaptation in a Temperate Tree Species

Highlights

- NSC stores in *P. trichocarpa* are heritable and locally adapted to climate
- Despite species-wide evolutionary potential in storage, populations are at risk
- Northern populations lack the genomic variants to evolve with climate change
- Southern populations have genomic diversity but face intense selective pressures

Authors

Meghan Blumstein, Andrew Richardson, David Weston, Jin Zhang, Wellington Muchero, Robin Hopkins

Correspondence

blumstein@fas.harvard.edu

In Brief

Blumstein et al. show variation in NSC storage in trees is heritable and locally adapted to climate. Despite species-wide evolutionary potential in storage, some populations are at risk. Northern populations lack genomic variants associated with high storage, while southern populations have these variants but face intense selective pressures.

Blumstein et al., 2020, Current Biology *30*, 1–7
April 20, 2020
https://doi.org/10.1016/j.cub.2020.02.001

CellPress

Please cite this article in press as: Blumstein et al., A New Perspective on Ecological Prediction Reveals Limits to Climate Adaptation in a Temperate Tree Species, Current Biology (2020), https://doi.org/10.1016/j.cub.2020.02.001

Current Biology
Article

CellPress

A New Perspective on Ecological Prediction Reveals Limits to Climate Adaptation in a Temperate Tree Species

Meghan Blumstein,[1,6,*] Andrew Richardson,[2,3] David Weston,[4] Jin Zhang,[4] Wellington Muchero,[4] and Robin Hopkins[1,5]
[1]Department of Organismic and Evolutionary Biology, Harvard University, 26 Oxford Street, Cambridge, MA 02138, USA
[2]Center for Ecosystem Science and Society, Northern Arizona University, Flagstaff, AZ 86011, USA
[3]School of Informatics, Computing, and Cyber Systems, Northern Arizona University, Flagstaff, AZ 86011, USA
[4]Biosciences Division, Oak Ridge National Laboratory, Oak Ridge, TN 37831, USA
[5]The Arnold Arboretum, 1300 Centre Street, Boston, MA 02130, USA
[6]Lead Contact
*Correspondence: blumstein@fas.harvard.edu
https://doi.org/10.1016/j.cub.2020.02.001

SUMMARY

Forests absorb a large fraction of anthropogenic CO2 emission, but their ability to continue to act as a sink under climate change depends in part on plant species undergoing rapid adaptation. Yet models of forest response to climate change currently ignore local adaptation as a response mechanism. Thus, considering the evolution of intraspecific trait variation is necessary for reliable, long-term species and climate projections. Here, we combine ecophysiology and predictive climate modeling with analyses of genomic variation to determine whether sugar and starch storage, energy reserves for trees under extreme conditions, have the heritable variation and genetic diversity necessary to evolve in response to climate change within populations of black cottonwood (*Populus trichocarpa*). Despite current patterns of local adaptation and extensive range-wide heritable variation in storage, we demonstrate that adaptive evolution in response to climate change will be limited by a lack of heritable variation within northern populations and by a need for extreme genetic changes in southern populations. Our method can help design more targeted species management interventions and highlights the power of using genomic tools in ecological prediction to scale from molecular to regional processes to determine the ability of a species to respond to future climates.

INTRODUCTION

Rates of forest tree mortality are increasing across large regions of the globe as a result of shifting drought regimes, extreme temperatures, and pest outbreaks associated with global change [1–4]. The rise in number and intensity of these climate-related selective pressures means adaptive evolution from local standing heritable variation will be a core component of species persistence strategies, along with migration and acclimation via plasticity [5, 6]. Adaptive evolution is particularly important, as tree populations already exhibit a high degree of local adaptation [7–9]. Despite high gene flow and long generation times [10], tree populations are able to undergo rapid adaptation, as evidenced by the paleoecological record following glaciation [11, 12]. Furthermore, plasticity and migration are unlikely to keep pace with climate change. Plastic variation may help plants temporarily acclimate to new climates, but studies have demonstrated that plastic variation may not be enough to cope with predicted change [13, 14] or may even be maladaptive [15]. In addition, migration rates may be limited due to dispersal rates and dispersal barriers [16, 17]. Thus, adaptation is a critical pillar of plant response to climate yet one that is often ignored in our species projections, despite its demonstrated improvement of models [18, 19].

Adaptive response is dependent on both the extent of heritable variation underlying an adaptive trait as well as the magnitude of evolutionary change necessary to meet the demands of unprecedented environmental change. Therefore, adaptive alleles must both be present in a population and be at appreciable allele frequencies to allow rapid evolution in response to rising temperatures and shifting precipitation patterns. Without the intraspecific trait variation necessary to evolve, populations will be at risk of local extinction [20–22]. To predict whether a species will be able to adapt to future climate, we must first identify a trait that is in fact adaptive, second quantify the amount and geographic distribution of heritable variation in the trait, third identify the genomic loci and subsequent alleles underlying the trait, and fourth assess the potential for these alleles to undergo local adaptive evolution [6, 9, 23, 24]. Here, we take these four steps to determine the potential for black cottonwood (*Populus trichocarpa*) to adapt to climate change through the evolution of variation in sugar and starch storage, hereafter referred to as nonstructural carbohydrate (NSC) storage.

The storage of NSCs has been hypothesized to be a key trait in providing resilience to trees under stress [25–27]. NSCs are labile sugars and starches stored in the parenchyma cells of woody tissues (stems, roots, etc.) in plants [28, 29]. They can be stored on the order of days to decades and support metabolic processes in the dormant season as well as initiate leaf out in the spring

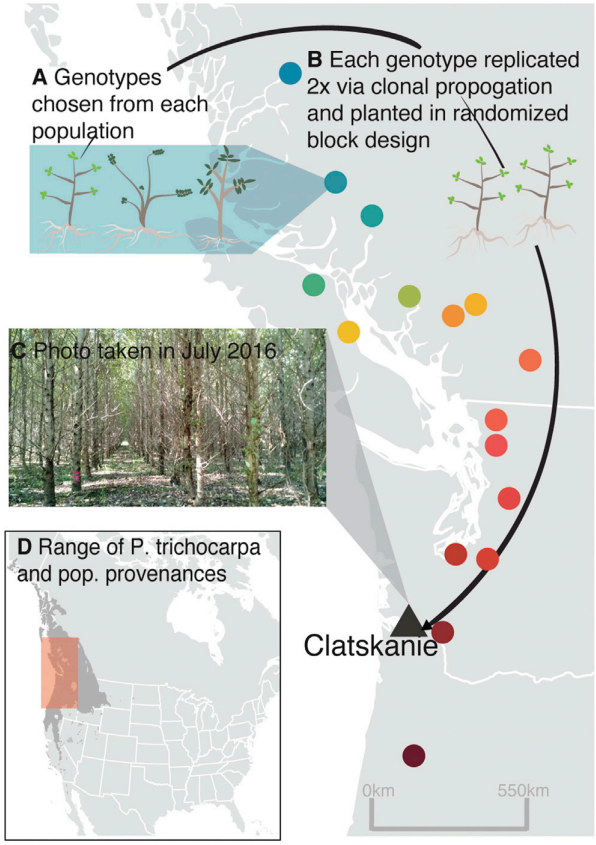

Figure 1. Common Garden Study Design

(A–C) Genotypes were (A) taken from each of 16 populations and (B) replicated twice via clonal propagation before being planted out in randomized blocks in the garden in Clatskanie, OR, as pictured in (C). Populations are color coded from cool to warm along a north-south axis.

(D) A map depicting the range of black cottonwood (*Populus trichocarpa*) and the subset of the range from which ramets were collected for planting in the common garden (black triangle).

[30]. NSC storage has also recently been thought to serve as a long-term "savings bank" for trees by allowing them to store energy in excess of their base demands in case future environmental extremes limit photosynthesis [25–27]. Under this hypothesis, plants would store more NSCs than needed in a normal year, which then act as an osmotic metabolic or defense buffer for trees growing in more stressful environments [26, 31]. Thus, plants growing in variable or extreme environments would be predicted to be locally adapted to store more than their counterparts in more ideal environments.

Recent studies on NSC storage have focused on the question of whether or not plants can tap into their stores and prolong life under stress. Many experimental and observational drought [32–34] and defoliation studies [35, 36] have demonstrated that plants can indeed draw down their NSC reserves under stress to sustain life under certain conditions (i.e., drought or shade), although some results are equivocal [37]. In addition, an experimental study of 10 tropical species has demonstrated a positive relationship between NSC storage and survival under drought, demonstrating that individuals who store *more* NSCs had higher stem water potentials and lived longer under stress [27]. Finally, interspecific studies indicate that average NSC storage can differ by up to 100% between species, indicating a potential genetic basis for the trait [38]. Together, these studies demonstrate that NSC stores, and more of them, can confer resilience under similar photosynthetically limiting stress, as predicted with climate change. However, no study to date has looked at variation within a species or across populations.

To evaluate the extent to which NSC storage is locally adapted and can continue to evolve in response to rapid climate change, we used a Department of Energy (DOE) common garden of black cottonwood (*Populus trichocarpa*) in Eastern Oregon [39]. We sampled both aboveground (stem) and belowground (root) woody tissues from 316 individuals, representing 242 genotypes and 16 populations (Figure 1), to measure heritable variation in NSC storage and find loci associated with the trait. We sampled during the dormant season (January), when the phloem is largely inactive [40, 41] and NSC variation is not impacted by variable fresh photosynthates. We then used the larger dataset of 860 re-sequenced genomes across 16 populations to make inferences about the evolutionary potential of NSC storage [39, 42].

RESULTS AND DISCUSSION

NSC Storage Is Heritable

Black cottonwoods have the NSC storage variation necessary for adaptive evolution. There is extensive total and heritable variation in aboveground (mean = 15.6 $mg \cdot g^{-1}$; σ_{Total} = 6.0 $mg \cdot g^{-1}$ NSC; $\sigma_{Heritable}$ = 2.8 $mg \cdot g^{-1}$ NSC) and belowground tissues (mean = 24.3 $mg \cdot g^{-1}$; σ_{Total} = 10.0 $mg \cdot g^{-1}$ NSC; $\sigma_{Heritable}$ = 3.6 $mg \cdot g^{-1}$ NSC). Roots store, on average, 1.6 ± 0.3 times higher concentrations of NSCs, which is consistent with other studies [38, 43]. By comparing genetic to total variation, we demonstrate significant broad-sense heritability underlying both aboveground and belowground NSC storage concentrations (Figure 1; $H^2_{aboveground}$ = 0.43 ± 0.1; $H^2_{belowground}$ = 0.32 ± 0.1), indicating that approximately 1/3 to 1/2 of variation measured in the garden could be passed onto offspring. NSC heritability is higher than most other physiological traits measured in the garden ($H^2_{Physiolgy\ Traits}$ = 0.26 ± 0.18) [44] and is on par with other traits thought to be associated with climate adaptation, such as relative growth rate (H^2_{Growth} = 0.42 ± 0.1). However, we found no heritability of variation in the ratio of above- to belowground storage concentrations ($H^2_{A/B}$ = 0.04 ± 0.0).

The amount of heritable variation in NSC storage is notable, with ranges spanning several percentage points for both aboveground (0.5%–3%; Δ 2.5%) and belowground (1%–4%; Δ 3%) storage. This variation is biologically meaningful, as even a 2%–4% increase in NSC storage can prolong lifespan of tree seedlings up to 9 days under experimental drought conditions [27]. Black cottonwood trees are riverine species and highly sensitive to changes in water level [45, 46], and Northwestern North America is projected to become drier over the next 100 years, with a significant decrease in the snowpack and precipitation that maintains river water levels [47]. Thus, the ability to evolve higher NSC storage concentrations as a back-up fuel source

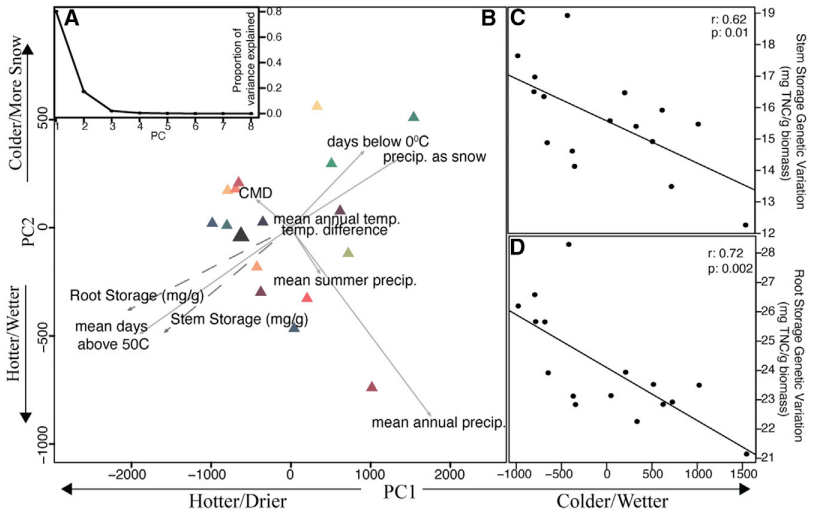

Figure 2. Population-Level Genetic Variation in NSC Storage Compared to the Climate of Origin

(A) A principle components analysis (PCA) of climate variables; the majority of the variance (81%) among site climate variables can be explained by PC1.

(B) Climate variables represent 30-year normal of parameters describing dryness and temperature, with PC1 largely indicating a gradient from wet and cool in the positive values to hot and dry in the negative range, although PC2 represents a gradient from warm and wet in the negative values to cold and dry in the positive values. Each population's current climate (triangle) and the site of the common garden (large gray triangle) are indicated. Population color varies from red in the South to blue in the North as in Figure 1.

(C and D) The results of a correlation analysis between PC1 and (C) above- and (D) belowground population-level heritable variation in NSC storage concentrations are presented on the right.

or a pool for maintaining hydraulic function could be a crucial survival trait for trees [48].

Climate Shapes NSC Storage

To determine the extent to which variation in NSCs are locally adapted and shaped by selection, we compare the heritable trait variation to the neutral genetic variation across populations. Specifically, we calculate the quantitative genetic trait differentiation among populations (Q_{st}) and compared this to the genomic differentiation at neutral sites among populations (F_{st}) [49] (mean; 95% credible interval; aboveground: Q_{st} = 0.31, 0.12–0.56; belowground: Q_{st} = 0.30, 0.11–0.57; [mean ± SD] F_{st} = 0.17 ± 0.06). Among populations, NSC storage variation significantly exceeds background genomic variation in both above and belowground NSC storage, supporting that divergence in NSC storage between populations is driven by natural selection (Wilcoxon test; aboveground: W = 18,675,000, $p < 0.001$; belowground: W = 17,894,000, $p < 0.001$).

Heritable variation in NSC storage is highly correlated with major environmental gradients across the range of black cottonwood, indicating local adaptation. We used a principal-component analysis (PCA) to reduce the dimensionality of and control for collinearity among relevant climate variables (Figures 2 and 3). The first PC describes an axis of colder/wetter to hotter/drier climates and is significantly correlated with heritable variation in both above- and belowground NSC storage (Figures 2 and 3; aboveground: d.f. = 14, r = 0.62, p = 0.01; belowground: d.f. = 14, r = 0.72, p = 0.002).

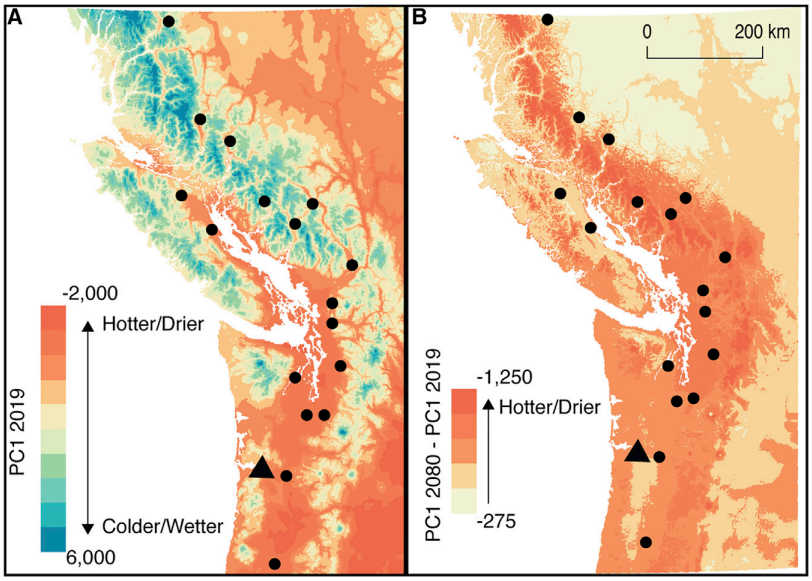

Figure 3. Current and Future Climate of Western North America Mapped in PC1 Space

Maps of (A) climatic variation along PC1 of present-day climate (2019) and (B) the difference along the climatic PC1 axis between the CCSM3 A1B future climate projections (2080) and the present-day climate. Dots represent populations, and the triangle is the location of the common garden in Clatskanie. The entire region is predicted to move in the more negative direction along PC1 (i.e., hotter and drier), with larger changes (darker color) occurring at high elevation and more southerly sites.

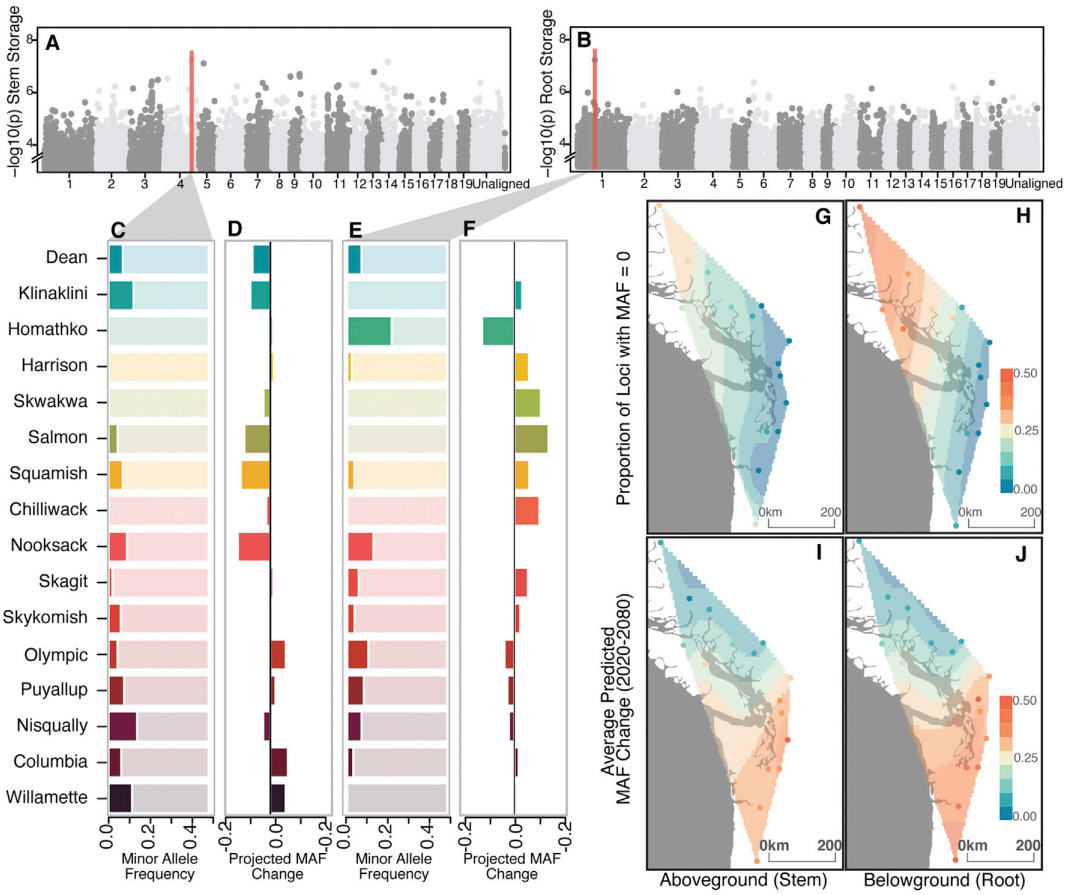

Figure 4. Using GWAS Results to Assess Adaptive Potential

(A and B) Genome-wide analysis study (GWAS) results for (A) aboveground and (B) belowground total NSC storage.

(C–F) The minor allele frequency (MAF) for the most significant loci in each GWAS (highlighted via a red line) is plotted for each population and 1,060 genomes (C and E), with the plots directly adjacent (D and F) showing the predicted change in MAF over the next 60 years due to climate change (IPCC A1B scenario).

(G and H) The top row of maps illustrate the proportion of loci associated with (G) aboveground and (H) belowground NSC storage that entirely lack the minor allele altogether (e.g., plot C and plot E; population Skwakwa), with warm colors lacking heritable variation. The bottom row of maps illustrates the average amount of absolute MAF change predicted under future climate scenarios, with warmer colors requiring greater allele frequency shifts.

See also Table S1 and Figures S2 and S4.

Individuals originating from hotter-drier environments have greater storage, lending support to the hypothesized relationship between environmental stress and NSC storage [25, 32], although, in black cottonwood, it is difficult to isolate the effect of latitude and subsequently phenological timing from climate. Further, NSC variation is largely uncorrelated with heritable variation in stem diameter (Figure S1; aboveground: m = 0.02, r = 0.13, p = 0.15; belowground: m = 0.03, r = 0.22, p = 0.04), suggesting that storage is genetically independent of growth. The geographic patterns of heritable variation in NSC storage are consistent with trees living at the extreme edge of their environmental tolerance evolving an adaptive "bet-hedging" strategy, although additional experiments teasing apart climate variables, mean versus variance in climate metrics, and phenology are needed to hone in on the precise climate drivers of local adaptation in storage.

Low Evolutionary Potential under Climate Change due to Allele Frequency Distributions

Given the existence of heritable variation in NSC storage, we used a genome-wide association study (GWAS) to identify candidate loci underlying storage. We find 209 SNPs above our inclusion cutoff from 111 genes associated with aboveground NSC storage and 86 SNPs from 50 genes associated with belowground storage (Figure 4A, 4B, and S2). Aboveground loci are enriched for several biological and molecular process gene ontology (GO) terms, such as carbohydrate metabolic process and catalytic activity, although belowground loci are enriched in functions such as transport (Figure S3). In both analyses, several genes associated with carbohydrate synthesis and transport were highlighted by our analysis (Table S1). All subsequent analyses were replicated using both the complete set of associated SNPs as well as a representative candidate

SNP for each unique gene; both show qualitatively similar results.

Our goal is to determine whether there is available local heritable variation at loci associated with variation in NSC storage that will allow for rapid evolution in response to climate change. We assess the current distribution of allele frequencies across populations by calculating the minor allele frequency (MAF), or proportion of individuals with the less common allele, within each population for each locus associated with aboveground or belowground NSC storage. This analysis uses the full DOE set of 860 resequenced black cottonwood genomes. We then transform our 30-year climate normal data, which represent the current conditions, into PC space and statistically associate the climate with population-level allele frequencies using a canonical-correlation analysis (CCA), which tests associations between two sets of multivariate variables [50] (Figure 3). We used the correlations between allele frequency and current climate to predict allele patterns under future climate conditions. Specifically, we used 2,080 projected climate conditions [47] transformed into PC space for each of our sampled populations to predict the expected MAF at each locus that would allow for current levels of local adaptation under future conditions (e.g., Figure 4C–4F; IPCC A1B scenario, CSM4 model). We also found our results to be robust to other climate models (Figure S4; IPCC A1B, CMIP3 23 model ensemble).

Populations at the edges of the black cottonwood range are vulnerable to extinction over the next 60 years due to insufficient heritable variation required for adaptive evolution to climate change. At the northern range limit, populations are entirely missing alleles associated with greater storage; up to 50% of loci within a population lack the allelic variation necessary to respond to warmer and drier climates (Figure 4G and 4H). This is concerning, given evidence that migration is unlikely to keep pace with rapid warming [16, 17]. However, our results do present opportunities for genetic rescue by identifying the target populations and alleles for use in assisted migration. Genetic rescue, or the migration of adaptive alleles into a population, has enabled rapid adaptation in several animal species (reviewed in [51]), and an assisted migration program is already in effect for the tree species larch [52].

In contrast, southern populations tend to contain the alleles associated with warmer/drier conditions, but these populations require extreme changes in allele frequency to adapt to future climate conditions. MAFs at populations below 50° latitude are predicted to shift in frequency Δ0.25–0.5 on average, although northern populations' frequencies are only projected to shift Δ0.03–0.12 on average (Figure 4I and 4J). The cost of the required selection in southern populations could result in local extinctions, as the number of individuals that may die could cause populations to drop below sustainable numbers [20, 22, 53, 54]. If the size of a population is reduced below a critical level, it becomes highly susceptible to extinction by demographic stochasticity, even if the genetic capacity to adapt to new environmental conditions is present in the population [20, 22, 53]. Given the rapidity of change is likely to outstrip generation time in *populus* (10–15 years to reproductive maturity), phenotypic plasticity may be key in ameliorating the short-term impacts of climate selection on southern populations [55, 56]. Future studies should examine the degree of plasticity in NSC storage and the environmental conditions that may induce higher storage.

Conclusions

We demonstrate the power of incorporating genomic data and an evolutionary perspective with plant physiology to scale from molecular measurements to regional predictions and thus better understand species response to climate change. Black cottonwood populations have locally adapted to climate through variation in NSC storage. However, despite extensive range-wide heritable intraspecific variation in storage, a lack of allelic variation locally will significantly limit the ability of this species to rapidly evolve in response to climate change. We reveal nuances in what is required for adaptation to occur across the range of a species that should inform how we design species management interventions and bring a new perspective to ecological prediction.

STAR★METHODS

Detailed methods are provided in the online version of this paper and include the following:

- KEY RESOURCES TABLE
- LEAD CONTACT AND MATERIALS AVAILABILITY
- EXPERIMENTAL MODEL AND SUBJECT DETAILS
- METHOD DETAILS
  - Field Collection
  - NSC Laboratory Preparation
- QUANTIFICATION AND STATISTICAL ANALYSIS
  - Spatial Autocorrelation
  - Statistical Model
  - Heritability, Q_{st}, and F_{st}
  - Climate
  - Genome-Wide Association Study & Gene Ontology
  - Minor Allele Frequency Projections
- DATA AND CODE AVAILABILITY

SUPPLEMENTAL INFORMATION

Supplemental Information can be found online at https://doi.org/10.1016/j.cub.2020.02.001.

ACKNOWLEDGMENTS

We thank M.E. Furze, C.F. White, D.L. Des Marais, N.M. Holbrook, and N. Freidman for comments and A. Viser, L. Gunter, E. Borjigin-Wang, and A. Chan for lab assistance. This material is based upon work supported by the US Department of Energy, Office of Science, Office of Workforce Development for Teachers and Scientists, Office of Science Graduate Student Research (SCGSR) program; by the National Science Foundation Graduate Research Fellowship under grant no. DGE1745303; and the Explorer's Club. The SCGSR program is administered by the Oak Ridge Institute for Science and Education (ORISE) for the DOE. ORISE is managed by ORAU under contract number DE-SC0014664.

AUTHOR CONTRIBUTIONS

Conceptualization, M.B., A.R., and R.H.; Data Collection/Processing, M.B., GWAS, J.Z., and W.M.; Statistical Analysis and Modeling, M.B.; Writing, M.B. and R.H.; Review and Editing, M.B., A.R., D.W., J.Z., W.M., and R.H.

DECLARATION OF INTERESTS

The authors declare no competing interests.

Received: October 29, 2019
Revised: December 17, 2019
Accepted: February 3, 2020
Published: March 26, 2020

REFERENCES

1. Allen, C.D., Macalady, A.K., Chenchouni, H., Bachelet, D., McDowell, N., Vennetier, M., Kitzberger, T., Rigling, A., Breshears, D.D., Hogg, E.H., et al. (2010). A global overview of drought and heat-induced tree mortality reveals emerging climate change risks for forests. For. Ecol. Manage. *259*, 660–684.
2. McDowell, N., Allen, C.D., Anderson-Teixeira, K., Brando, P., Brienen, R., Chambers, J., Christoffersen, B., Davies, S., Doughty, C., Duque, A., et al. (2018). Drivers and mechanisms of tree mortality in moist tropical forests. New Phytol. *219*, 851–869.
3. Anderegg, W.R., Hicke, J.A., Fisher, R.A., Allen, C.D., Aukema, J., Bentz, B., Hood, S., Lichstein, J.W., Macalady, A.K., McDowell, N., et al. (2015). Tree mortality from drought, insects, and their interactions in a changing climate. New Phytol. *208*, 674–683.
4. Anderegg, W.R., Klein, T., Bartlett, M., Sack, L., Pellegrini, A.F., Choat, B., and Jansen, S. (2016). Meta-analysis reveals that hydraulic traits explain cross-species patterns of drought-induced tree mortality across the globe. Proc. Natl. Acad. Sci. USA *113*, 5024–5029.
5. Aitken, S.N., Yeaman, S., Holliday, J.A., Wang, T., and Curtis-McLane, S. (2008). Adaptation, migration or extirpation: climate change outcomes for tree populations. Evol. Appl. *1*, 95–111.
6. Sork, V.L., Aitken, S.N., Dyer, R.J., Eckert, A.J., Legendre, P., and Neale, D.B. (2013). Putting the landscape into the genomics of trees: approaches for understanding local adaptation and population responses to changing climate. Tree Genet. Genomes *9*, 901–911.
7. Savolainen, O., Pyhäjärvi, T., and Knürr, T. (2007). Gene flow and local adaptation in trees. Annu. Rev. Ecol. Evol. Syst. *38*, 595–619.
8. Borkowski, D.S., Hoban, S.M., Chatwin, W., and Romero-Severson, J. (2017). Rangewide population differentiation and population substructure in *Quercus rubra* L. Tree Genet. Genomes *13*, 67.
9. Alberto, F.J., Aitken, S.N., Alía, R., González-Martínez, S.C., Hänninen, H., Kremer, A., Lefèvre, F., Lenormand, T., Yeaman, S., Whetten, R., and Savolainen, O. (2013). Potential for evolutionary responses to climate change - evidence from tree populations. Glob. Change Biol. *19*, 1645–1661.
10. Kremer, A., Ronce, O., Robledo-Arnuncio, J.J., Guillaume, F., Bohrer, G., Nathan, R., Bridle, J.R., Gomulkiewicz, R., Klein, E.K., Ritland, K., et al. (2012). Long-distance gene flow and adaptation of forest trees to rapid climate change. Ecol. Lett. *15*, 378–392.
11. Davis, M.B., and Shaw, R.G. (2001). Range shifts and adaptive responses to Quaternary climate change. Science *292*, 673–679.
12. Davis, M.B., Shaw, R.G., and Etterson, J.R. (2005). Evolutionary responses to changing climate. Ecology *86*, 1704–1714.
13. Duputié, A., Rutschmann, A., Ronce, O., and Chuine, I. (2015). Phenological plasticity will not help all species adapt to climate change. Glob. Change Biol. *21*, 3062–3073.
14. Franks, S.J. (2011). Plasticity and evolution in drought avoidance and escape in the annual plant Brassica rapa. New Phytol. *190*, 249–257.
15. Hendry, A.P. (2016). Key questions on the role of phenotypic plasticity in eco-evolutionary dynamics. J. Hered. *107*, 25–41.
16. Zhu, K., Woodall, C.W., and Clark, J.S. (2012). Failure to migrate: lack of tree range expansion in response to climate change. Glob. Change Biol. *18*, 1042–1052.
17. McLachlan, J.S., Clark, J.S., and Manos, P.S. (2005). Molecular indicators of tree migration capacity under rapid climate change. Ecology *86*, 2088–2098.
18. Cotto, O., Wessely, J., Georges, D., Klonner, G., Schmid, M., Dullinger, S., Thuiller, W., and Guillaume, F. (2017). A dynamic eco-evolutionary model predicts slow response of alpine plants to climate warming. Nat. Commun. *8*, 15399.
19. Valladares, F., Matesanz, S., Guilhaumon, F., Araújo, M.B., Balaguer, L., Benito-Garzón, M., Cornwell, W., Gianoli, E., van Kleunen, M., Naya, D.E., et al. (2014). The effects of phenotypic plasticity and local adaptation on forecasts of species range shifts under climate change. Ecol. Lett. *17*, 1351–1364.
20. Allaby, R.G., Kitchen, J.L., and Fuller, D.Q. (2016). Surprisingly low limits of selection in plant domestication. Evol. Bioinform. Online *11* (*Suppl 2*), 41–51.
21. Polechová, J., and Barton, N.H. (2015). Limits to adaptation along environmental gradients. Proc. Natl. Acad. Sci. USA *112*, 6401–6406.
22. Smith, J.M. (1968). "Haldane's dilemma" and the rate of evolution. Nature *219*, 1114–1116.
23. Anderson, J.T., Inouye, D.W., McKinney, A.M., Colautti, R.I., and Mitchell-Olds, T. (2012). Phenotypic plasticity and adaptive evolution contribute to advancing flowering phenology in response to climate change. Proc. Biol. Sci. *279*, 3843–3852.
24. Anderegg, W.R.L. (2015). Spatial and temporal variation in plant hydraulic traits and their relevance for climate change impacts on vegetation. New Phytol. *205*, 1008–1014.
25. McDowell, N., Pockman, W.T., Allen, C.D., Breshears, D.D., Cobb, N., Kolb, T., Plaut, J., Sperry, J., West, A., Williams, D.G., and Yepez, E.A. (2008). Mechanisms of plant survival and mortality during drought: why do some plants survive while others succumb to drought? New Phytol. *178*, 719–739.
26. Sala, A., Piper, F., and Hoch, G. (2010). Physiological mechanisms of drought-induced tree mortality are far from being resolved. New Phytol. *186*, 274–281.
27. O'Brien, M.J., Reynolds, G., Ong, R., and Hector, A. (2017). Resistance of tropical seedlings to drought is mediated by neighbourhood diversity. Nat. Ecol. Evol. *1*, 1643–1648.
28. Chapin, F.S., III, Schulze, E., and Mooney, H.A. (1990). The ecology and economics of storage in plants. Annu. Rev. Ecol. Syst. *21*, 423–447.
29. Plavcová, L., and Jansen, S. (2015). The role of xylem parenchyma in the storage and utilization of nonstructural carbohydrates. In Functional and Ecological Xylem Anatomy, U. Hacke, ed. (Springer), pp. 209–234.
30. Hartmann, H., and Trumbore, S. (2016). Understanding the roles of nonstructural carbohydrates in forest trees - from what we can measure to what we want to know. New Phytol. *211*, 386–403.
31. McDowell, N.G., and Sevanto, S. (2010). The mechanisms of carbon starvation: how, when, or does it even occur at all? New Phytol. *186*, 264–266.
32. Sevanto, S., McDowell, N.G., Dickman, L.T., Pangle, R., and Pockman, W.T. (2014). How do trees die? A test of the hydraulic failure and carbon starvation hypotheses. Plant Cell Environ. *37*, 153–161.
33. Quirk, J., McDowell, N.G., Leake, J.R., Hudson, P.J., and Beerling, D.J. (2013). Increased susceptibility to drought-induced mortality in Sequoia sempervirens (Cupressaceae) trees under Cenozoic atmospheric carbon dioxide starvation. Am. J. Bot. *100*, 582–591.
34. Hartmann, H., Ziegler, W., and Trumbore, S. (2013). Lethal drought leads to reduction in nonstructural carbohydrates in Norway spruce tree roots but not in the canopy. Funct. Ecol. *27*, 413–427.
35. Landhäusser, S.M., and Lieffers, V.J. (2012). Defoliation increases risk of carbon starvation in root systems of mature aspen. Trees *26*, 653–661.
36. Piper, F.I., and Fajardo, A. (2014). Foliar habit, tolerance to defoliation and their link to carbon and nitrogen storage. J. Ecol. *102*, 1101–1111.

37. Adams, H.D., Zeppel, M.J.B., Anderegg, W.R.L., Hartmann, H., Landhäusser, S.M., Tissue, D.T., Huxman, T.E., Hudson, P.J., Franz, T.E., Allen, C.D., et al. (2017). A multi-species synthesis of physiological mechanisms in drought-induced tree mortality. Nat. Ecol. Evol. *1*, 1285–1291.
38. Furze, M.E., Huggett, B.A., Aubrecht, D.M., Stolz, C.D., Carbone, M.S., and Richardson, A.D. (2019). Whole-tree nonstructural carbohydrate storage and seasonal dynamics in five temperate species. New Phytol. *221*, 1466–1477.
39. Slavov, G.T., DiFazio, S.P., Martin, J., Schackwitz, W., Muchero, W., Rodgers-Melnick, E., Lipphardt, M.F., Pennacchio, C.P., Hellsten, U., Pennacchio, L.A., et al. (2012). Genome resequencing reveals multiscale geographic structure and extensive linkage disequilibrium in the forest tree Populus trichocarpa. New Phytol. *196*, 713–725.
40. Aloni, R., Raviv, A., and Peterson, C.A. (1991). The role of auxin in the removal of dormancy callose and resumption of phloem activity in *Vitis vinifera*. Can. J. Bot. *69*, 1825–1832.
41. Bowen, M.R., and Hoad, G.V. (1968). Inhibitor content of phloem and xylem sap obtained from willow (Salix viminalis L.) entering dormancy. Planta *81*, 64–70.
42. Tuskan, G.A., Difazio, S., Jansson, S., Bohlmann, J., Grigoriev, I., Hellsten, U., Putnam, N., Ralph, S., Rombauts, S., Salamov, A., et al. (2006). The genome of black cottonwood, Populus trichocarpa (Torr. & Gray). Science *313*, 1596–1604.
43. Richardson, A.D., Carbone, M.S., Keenan, T.F., Czimczik, C.I., Hollinger, D.Y., Murakami, P., Schaberg, P.G., and Xu, X. (2013). Seasonal dynamics and age of stemwood nonstructural carbohydrates in temperate forest trees. New Phytol. *197*, 850–861.
44. McKown, A.D., Guy, R.D., Klápště, J., Geraldes, A., Friedmann, M., Cronk, Q.C., El-Kassaby, Y.A., Mansfield, S.D., and Douglas, C.J. (2014). Geographical and environmental gradients shape phenotypic trait variation and genetic structure in Populus trichocarpa. New Phytol. *201*, 1263–1276.
45. Rood, S.B., Braatne, J.H., and Hughes, F.M. (2003). Ecophysiology of riparian cottonwoods: stream flow dependency, water relations and restoration. Tree Physiol. *23*, 1113–1124.
46. Rood, S.B., and Mahoney, J.M. (1990). Collapse of riparian poplar forests downstream from dams in western praries: probable causes and prospects for mitigation. Environ. Manage. *14*, 451–464.
47. IPCC (2013). Climate Change 2013: The Physical Science Basis. Contribution of Working Group I to the Fifth Assessment Report of the Intergovernmental Panel on Climate Change (Cambridge University Press).
48. Sala, A., Woodruff, D.R., and Meinzer, F.C. (2012). Carbon dynamics in trees: feast or famine? Tree Physiol. *32*, 764–775.
49. Whitlock, M.C., and Gilbert, K.J. (2012). Q(ST) in a hierarchically structured population. Mol. Ecol. Resour. *12*, 481–483.
50. Hamann, A., Wang, T., Spittlehouse, D.L., and Murdock, T.Q. (2013). A comprehensive, high-resolution database of historical and projected climate surfaces for western North America. Bull. Am. Meteorol. Soc. *94*, 1307–1309.
51. Whiteley, A.R., Fitzpatrick, S.W., Funk, W.C., and Tallmon, D.A. (2015). Genetic rescue to the rescue. Trends Ecol. Evol. *30*, 42–49.
52. O'Neill, G.A., Ukrainetz, N.K., Carlson, M., Cartwright, C.V., Jaquish, B.C., King, J.N., Krakowski, J., Russell, J.H., Stoehr, M.U., Xie, C.-Y., et al. (2008). Assisted migration to address climate change in British Columbia: recommendations for interim seed transfer standards. Volume Tech. Rep. *48*, B.C. Ministry of Forestry.
53. Haldane, J.B.S. (1957). The cost of natural selection. J. Genet. *55*, 511–524.
54. Lindsey, H.A., Gallie, J., Taylor, S., and Kerr, B. (2013). Evolutionary rescue from extinction is contingent on a lower rate of environmental change. Nature *494*, 463–467.
55. O'Connor, M.I., Selig, E.R., Pinsky, M.L., and Altermatt, F. (2012). Toward a conceptual synthesis for climate change responses. Glob. Ecol. Biogeogr. *21*, 693–703.
56. Matesanz, S., Gianoli, E., and Valladares, F. (2010). Global change and the evolution of phenotypic plasticity in plants. Ann. N Y Acad. Sci. *1206*, 35–55.
57. R Core Development Team (2018). R: A language and environment for statistical computing (R Foundation for Statistical Computing).
58. Zhang, J., Yang, Y., Zheng, K., Xie, M., Feng, K., Jawdy, S.S., Gunter, L.E., Ranjan, P., Singan, V.R., Engle, N., et al. (2018). Genome-wide association studies and expression-based quantitative trait loci analyses reveal roles of HCT2 in caffeoylquinic acid biosynthesis and its regulation by defense-responsive transcription factors in Populus. New Phytol. *220*, 502–516.
59. Carpenter, B., Gelman, A., Hoffman, M.D., Lee, D., Goodrich, B., Betancourt, M., Brubaker, M., Guo, J., Li, P., and Riddell, A. (2017). Stan: a probabalistic programming language. J. Stat. Softw. *76*, 1–32.
60. Oksanen, J., Blanchet, F.G., Friendly, M., Kindt, R., Legendre, P., McGlinn, D., Minchin, P.R., O'Hara, R.B., Simpson, G.L., Solymos, P., et al. (2019). vegan: Community Ecology Package. https://cran.r-project.org/web/packages/vegan/index.html.
61. Nychka, D., Furrer, R., Paige, J., and Sain, S. (2017). fields: Tools for spatial data (University Corporation for Atmospheric Research).
62. Alexa, A., and Rahnenfuhrer, J. (2019). topGO: Enrichment analysis for gene ontology. https://bioconductor.org/packages/release/bioc/html/topGO.html.
63. Falcon, S., and Gentleman, R. (2007). Using GOstats to test gene lists for GO term association. Bioinformatics *23*, 257–258.
64. Evans, L.M., Slavov, G.T., Rodgers-Melnick, E., Martin, J., Ranjan, P., Muchero, W., Brunner, A.M., Schackwitz, W., Gunter, L., Chen, J.G., et al. (2014). Population genomics of Populus trichocarpa identifies signatures of selection and adaptive trait associations. Nat. Genet. *46*, 1089–1096.
65. Richardson, A.D., Carbone, M.S., Huggett, B.A., Furze, M.E., Czimczik, C.I., Walker, J.C., Xu, X., Schaberg, P.G., and Murakami, P. (2015). Distribution and mixing of old and new nonstructural carbon in two temperate trees. New Phytol. *206*, 590–597.
66. Tixier, A., Orozco, J., Roxas, A.A., Earles, J.M., and Zwieniecki, M.A. (2018). Diurnal variation in nonstructural carbohydrate storage in trees: remobilization and vertical mixing. Plant Physiol. *178*, 1602–1613.
67. Chow, P.S., and Landhäusser, S.M. (2004). A method for routine measurements of total sugar and starch content in woody plant tissues. Tree Physiol. *24*, 1129–1136.
68. Landhäusser, S.M., Chow, P.S., Dickman, L.T., Furze, M.E., Kuhlman, I., Schmid, S., Wiesenbauer, J., Wild, B., Gleixner, G., Hartmann, H., et al. (2018). Standardized protocols and procedures can precisely and accurately quantify non-structural carbohydrates. Tree Physiol. *38*, 1764–1778.
69. Lamy, J.B., Delzon, S., Bouche, P.S., Alia, R., Vendramin, G.G., Cochard, H., and Plomion, C. (2014). Limited genetic variability and phenotypic plasticity detected for cavitation resistance in a Mediterranean pine. New Phytol. *201*, 874–886.
70. Spitze, K. (1993). Population structure in *Daphnia obtusa*: quantitative genetic and allozymic variation. Genetics *135*, 367–374.
71. Slater, L.J., Villarini, G., and Bradley, A.A. (2019). Evaluation of the skill of North-American Multi-Model Ensemble (NMME) Global Climate Models in predicting average and extreme precipitation and temperature over the continental USA. Clim. Dyn. *53*, 7381–7396.
72. Zhou, X., and Stephens, M. (2012). Genome-wide efficient mixed-model analysis for association studies. Nat. Genet. *44*, 821–824.

STAR★METHODS

KEY RESOURCES TABLE

REAGENT or RESOURCE	SOURCE	IDENTIFIER
Chemicals, Peptides, and Recombinant Proteins		
Acetic Acid	VWR	BDH20108.292
95% Ethanol	VWR	89125-180
Sodium Acetate	VWR	200004-240
Alpha-Amylase	Sigma Aldrich	A4551
Amyloglucosidase	Sigma Aldrich	1202332001
Phenol	VWR	BT135960-100G
Sulfuric Acid	VWR	BDH3072-2.5LG
PGO	Sigma Aldrich	P7119
O-dianisidine dihydrochloride	Sigma Aldrich	D3252
Deposited Data		
Total Nonstrucral Carbohydrate concentrations	This paper	https://github.com/blumsteinm/H2_Qst_Model
Populus trichocarpa sequence data	[42]	https://genome.jgi.doe.gov/portal/Poptr1_1/Poptr1_1.download.html
Climate Data of Western North America (WNA)	[50]	https://sites.ualberta.ca/~ahamann/data/climatewna.html
Software and Algorithms		
R v.3.5.1	[57]	https://www.r-project.org/
EMMAX	[58]	https://genome.sph.umich.edu/wiki/EMMAX
STAN/rstan v. 2.18.2	[59]	http://www.mc-stan.org
Vegan v.2.5-3 (R package)	[60]	https://cran.r-project.org/web/packages/vegan/vegan.pdf
Fields v.9.6	[61]	https://cran.r-project.org/web/packages/fields/index.html
Gamma hierarchical model	This paper	https://github.com/blumsteinm/H2_Qst_Model
topGO	[62]	https://bioconductor.org/packages/release/bioc/html/topGO.html
GOstats	[63]	https://bioconductor.org/packages/release/bioc/html/GOstats.html

LEAD CONTACT AND MATERIALS AVAILABILITY

Further information and requests for resources and reagents should be directed to and will be fulfilled by the lead contact, Meghan Blumstein (blumsteinm@gmail.com). All data and scripts generated by this study have been deposited in (https://github.com/blumsteinm/H2_Qst_Model).

EXPERIMENTAL MODEL AND SUBJECT DETAILS

Samples were collected from a Department of Energy black cottonwood (*Populus trichocarpa*) common garden, located near Clatskanie, Oregon (46.12°N, 123.27°W). The garden contains three randomized blocks of replicated genotypes along an East-West axis each containing 1,060 unique genotypes for a total of 3,180 individuals in each garden, which originate from 16 different provenances (referred to here as populations) (Figure 1). Population assignments were taken from a previous publication [64]. Plants in the garden received no extra water or nutrients after their establishment in the first year. The collection of each accession is described in Slavov et al. [39]. All individuals were planted in 2009, but one replicate was coppiced in the winter of 2013-2014, thus we only sampled from the two non-coppiced replicates where individuals were eight years old at the time of sampling

METHOD DETAILS

Field Collection

All samples were collected from January 6th to January 10th 2017, between 7a.m. and 4 p.m. While NSC concentrations are well known to fluctuate seasonally in predictable ways [38, 65], there is little evidence of diurnal fluctuations in total storage in woody

tissues, particularly in the dormant season. Carbohydrates may hydrolyze back and forth between sugar and starch over the course of the day in woody tissues, while the total amount of sugars remains largely unchanged [66]. However, to account for potential differences in time of sampling and microenvironment, we sampled in a randomized, hierarchical experimental design. The diameter at breast height (DBH) was also taken during this period, with the average measuring 155.2mm ± 46.9mm.

We collected above (stem) and below-ground (root) tissue using a 4.3mm increment borer (Haglöf Company Group, Långsele, Sweden). Stem tissue was taken at DBH and root tissue was taken from major coarse roots approximately 30cm away from the base of the tree. Samples were kept on dry ice in the field during collection, then shipped to Harvard University in Cambridge, MA and stored at −80°C.

Sampling was designed to collect a *minimum* of three unique genotypes (two replicates each) from each of the 16 populations, for a total of 96 initial trees sampled for assessment of heritability. An additional 220 individuals were collected to increase power for in the GWAS analysis for a total of 316 individuals from, representing 242 unique genotypes.

NSC Laboratory Preparation

We measured sugar and starch concentrations in the outer 2cm of the stem cores and outer 1.5cm of the root cores. Samples were first freeze-dried for 24-hours (FreeZone 2.5; Labconco, Kansas City, MO, and Hybrid Vacuum Pump, Vacuubrand, Wertheim, Germany), then ground to a fine powder (mesh 10, Thomas Scientific Wiley Mill, Swedesboro, NJ, USA; SPEX SamplePrep 1600; MiniG, Metuchen, NJ) and stored in sealed glass vials. Sugar and starch extraction protocols were adapted from [67]

Sugar was extracted from 10 mg of dried tissue using 80% hot ethanol, followed by a colorimetric assay with phenol and sulfuric acid, and read using a spectrophotometer at 490nm (Thermo Fisher Scientific GENESYS 10S UV-Vis, Waltham, MA). Sugar concentrations of mg sugar per g of dry wood were calculated using a 1:1:1 glucose-fructose-galactose standard curve (Sigma Chemicals, St. Louis, MO).

Starch was extracted using the tissue remaining after sugar extraction. Tissue was solubilized in NAOH, then incubated for 24-hours with alpha-amylase and amyloglucosidase digestive enzymes, which digested starch into glucose. Solutions were then assayed using a PGO-color reagent solution (Sigma chemicals) and read on the spectrophotometer at 525nm. Starch concentrations of mg glucose-starch-equivalent per g dry wood were calculated based on a glucose standard curve (Sigma Chemicals).

For all lab analyses, at least two internal laboratory standards were included (*Quercus rubrum* stemwood from Harvard Forest, MA; 42.01 ± 5.13 mg·g-1 Sugar, 30.17 ± 4.23 mg·g-1 starch). This acid methodology extracts all fructose, glucose, sucrose, and starch, as well as other oligosaccharides and other glucans [68]. We report these carbohydrates as one combined metric of Total Nonstructural Carbohydrates (TNC), representing sugar and starch concentrations added together.

QUANTIFICATION AND STATISTICAL ANALYSIS

Spatial Autocorrelation

Logged data were corrected for within-garden spatial autocorrelation using a thin-plate spline method (e.g., [64]), using the *fields* (9.6) package in *R* v.3.5.1 [57]. The model intercept was then added back to the residuals and then the exponential of these values was taken to place them back on a biologically meaningful scale.

Statistical Model

Given variation in our hierarchical sampling regime, we chose to use Bayesian hierarchical modeling to parse variation within and among populations. All statistical analyses were conducted in *R*, using the programming language *Stan* (http://www.mc-stan.org) [59], accessed via the *rstan* v.2.18.2 package. All model parameters were assigned noninformative priors (https://github.com/blumsteinm/H2_Qst_Model). We chose to treat both above and belowground stores as separate traits because they appear to vary independently in the literature [34, 35] and do not appear to tradeoff within other species [38] or across our populations. We also calculated the ratio of above to below-ground storage concentrations within trees and examined heritable variation in this trait. The ratio was calculated as the concentration of root storage minus the concentration of stem storage, divided by the larger of the two values.

Two different models were run to parse (1) the heritable variation and (2) the variation within and among populations (N_{stems} = 314, N_{roots} = 316). We chose to run two separate models for ease of extracting genetic variation values from the heritability model [e.g., 64, 69] The models took the form of the following hierarchical equations:

$$Y_{ig} = \alpha_g + \varepsilon_{ig} \quad (1)$$

$$Y_{igp} = \alpha_p + \alpha_{gp} + \varepsilon_{igp} \quad (2)$$

where *p* is population (i.e., provenance of genotype; N_{pop} = 16), g is genotype (N_g = 245), and *i* is individual. Both above and belowground data were modeled as a gamma distribution as they both had long right tails and no values at or below 0. The random effects outcomes (α's) of Equations 1 and 2 were estimated using 6,000 random draws from the posterior distribution of each equation respectively, using the mean value of draw as each parameter estimate. These estimates for the heritable variation in storage are

also known as the best linear unbiased predictions (BLUPs). This method was also repeated with our diameter measurements to calculate the heritable variation in DBH.

Heritability, Q_{st}, and F_{st}

Both broad-sense heritability (H^2) and phenotypic divergence (Q_{st}) were estimated using the Bayesian hierarchical model outputs. Each parameter required for the H^2 and Q_{st} estimates were drawn from the posterior distributions of both Equations 1 and 2 and used to calculate H^2 and Q_{st} 6,000 times (for each of the posterior draws), generating uncertainty bounds for each estimate. H^2 was calculated using the random effects variances from Equation 1 as:

$$\sigma^2_{Genotype} \Big/ \left(\sigma^2_{Genotype} + \sigma^2_{Microenvironment}\right) \quad (3)$$

Genotype variance was taken as the variance among replicates and microenvironmental variance was taken as the residual variance of the model. Q_{st} was calculated via the formula [49, 70]:

$$\sigma^2_{Population} \Big/ \left(2\sigma^2_{Genotype} + \sigma^2_{Population}\right) \quad (4)$$

F_{st} estimates were taken from previous work [64], where F_{st} was calculated in 1-kb windows as $(\pi_T\text{-}\pi_S)/\pi_T$; where π_T is SNP diversity across all individuals and π_S is weighted within-population SNP diversity. A nonparametric Wilcoxon t test was performed to test whether the distribution of F_{st} values and above and belowground Q_{st} posterior estimates significantly differed. All results are reported in text.

Climate

The past climatic data used to estimate clinal variation in NSC storage were climate-normal layers fit to western North America that represent 30-year normals (1961-1990) from climateWNA [50]. We chose this dataset in particular because the down-scaling routine is optimized for our study region and like-formatted (ie. scale and variables) climate projections were available for a multitude of GCMs and climate scenarios, allowing us to project the environmental clines we identified into future climate space. However, by using Normals data, we do lose many variables that go beyond means to capture climate stochasticity. All 26 available climate parameters were highly correlated, thus to reduce dimensionality and account for collinearity among our climatic variables, we used a principle components analysis (PCA) (Figure 2). Many climate parameters were found to be redundant in our PCA given their high correlation with other parameters and all parameters analyzed fell along a precipitation or temperature gradient. Thus, we chose to include only the 8 climate variables with the highest loading values on PC1 and PC2 in our analysis to simplify visualization (Figure 2).

We then fitted above and belowground NSC storage concentrations population-level heritable variation to the first two principle components of this ordination space using ''envfit'' from the *vegan* v.2.5-3 package [60] and patterns were further teased out using a linear regression of population-variation against PC1and PC2 as predictors (Figure 2, N = 16).

To get population-level estimates of future climate, we used down-scaled data representing the IPCC's A1B (moderate) emissions scenario from the National Center for Atmospheric Research's CCSM3 global climate model for the year 2080 from climateWNA [50]. We chose to run NCAR's CCSM3 model as it is part of the North American Multi-Model Ensemble and had available data on climateWNA. CCSM3 predictions are in line with other models in the North American Multi-Model Ensemble as well as the ensemble predictions [71]. Once acquired, we projected future climate predictions into the PC space fit with current climate and used these values to assess climate response (Figure 3). In addition, we repeated our analyses using ensemble data for all 23 CMIP3 models from climateWNA and found no significant differences in our predictions (Figure S4).

Genome-Wide Association Study & Gene Ontology

We performed a genome-wide association study (GWAS) on the spatial-autocorrelation corrected values of heritable variation for both above and belowground total NSC storage concentrations following the protocol of Zhang et al. [58] and the software *EMMAX* with a correction for kinship [72]. We utilized 8,253,066 SNP variants with dataset-wide minor allele frequencies > 0.05, from 917 accessions, using -log10(P) > = 5 as our inclusion cutoff (Figure 4). We also repeated analyses with more stringent multiple-testing FDR rate corrections (-log10 = 6 and 6.5) and found them to be robust, but chose to use the threshold of -log10 = 5 given the likely polygenic nature of the trait and to more robustly build predictive models. Our analysis uncovered several gene models within 6kb (the distance at which LD decays in populus [42]) of SNPs with p values above our inclusion cutoff with functions purportedly associated with carbohydrate synthesis, binding, and transport in both stems, such as Potri.001G134900, Potri.001G226600 and Potri.003G022900, and roots, such as Potri.006G122000, Potri.007G040700, Potri.011G110800 (Table S1). Gene models associated with the production/degradation of secondary compounds and lipids were also uncovered (Table S1). We then performed a gene ontology (GO) analysis to summarize these results, then aggregate results into GO slim categories (Figure S2). We used the packages *topGO* version 1.0 [62] and *GOstats* version 1.7.4 in R [63] and the *P. trichocarpa* v.3.1 annotation file from the DOE repository to conduct the analysis [42, 64].

Minor Allele Frequency Projections

At each locus associated with aboveground or belowground storage, we calculated the minor allele frequency (MAF) by population. We then generated a statistical association between the MAF of each population at each locus associated with NSC storage and the PCs defined in our previous climate analysis via a canonical correlation analysis (CCA) with 4,000 permutations, running above and belowground loci in separate analyses. CCA is a multivariate method commonly used in community ecology to establish relationships between biological assemblages of species and environment, where here each loci is acting like species. We checked the accuracy of our model by plotting predicted allele frequencies against actual by population, finding (Figure S3). We then predicted the expected population-level MAF at each locus given the CCA model and 2080 projected climate PCs for each population. Finally, to make interpolated maps of our population-level data for ease of viewing, we used a thin-plate spline method from the *fields v.9.6* package in *R [61]* (all results in Figure 4). We also repeated this analysis using genes with representative SNPs, meaning we chose the most significant SNP from each gene to use as the marker for each gene region.

DATA AND CODE AVAILABILITY

The datasets and code generated during this study are available on github (https://github.com/blumsteinm/H2_Qst_Model).

2

Trees actively allocate carbohydrates to storage

In Submission As:

Blumstein, MJ, A. Sala, D. Weston, M.N. Holbrook, R. Hopkins. *In Submission*. Trees actively allocate carbohydrates to storage.

Abstract

Whether the storage of nonstructural carbohydrates (NSCs) by plants is a passive or active process is a central question in understanding carbon allocation strategies and predicting future plant productivity[11,13,30,31]. To date, evidence for passive versus active storage is equivocal as studies fail to simultaneously test both assumptions underlying active storage (eg.[11,32]): that it is (1) under genetic control and (2) allocated to at the expense of other sinks[13]. Building off recent data demonstrating that variation in NSC storage is heritable[33], here we test whether genetic variation in NSC storage trades off with genetic variation in other carbon sinks within a temperate tree species. To test the active storage hypotheses, we measured genetic variation in seven traits related to carbon supply, defense, growth and storage within a common garden of black cottonwood *(Populus trichocarpa)* and searched for tradeoffs amongst them. We find allocation tradeoffs between individual's investment in growth and defense versus storage once differences in productivity are accounted for, demonstrating that NSC reserve formation is an active process. Furthermore, we found that individuals who invest less in growth and defense can store up to 8-10 mg/g, or ~30%, more NSCs in their tissues then their counterparts, a sum that may be critical for tree survival under novel climate regimes. Our results suggest a paradigm shift in the way we conceptualize and model carbon allocation to storage in tree species.

Body Text

The storage of nonstructural carbohydrates (NSCs) is essential for long-lived, immobile tree species. NSC stores serve as a savings bank for trees by providing energetic reserves for both predictable and unpredictable carbon supply fluctuations (eg. night, dormant season, environmental disturbance)[9,13]. Higher NSC stores can prolong life under drought conditions[34] and may enable trees to withstand stochastic environmental events, such as intense freeze-thaws, and herbivory[11,30,32,35]. Climate induced

changes in drought and herbivory cycles are already causing episodes of large-scale tree mortality (eg. [3]); thus it is important to better predict if and how trees may tolerate and eventually evolve under variable environments. Increasing NSC storage will likely benefit individuals living in temporally stochastic environments, and yet, it is still unclear if trees actively control the amount of carbon allocated to storage versus other carbon sinks such as growth. Is the underlying process of reserve carbon formation passive or active[11,13,30,31]?

Establishing the extent to which variation in NSCs are due to a passive or active allocation of resources is fundamental for determining how forests will physiologically respond to and evolve in response to climate change, human disturbance, and stress. The passive model of storage assumes that any accumulation of NSCs only occurs after the priority sink demands of growth, defense, respiration, and reproduction have all been satisfied[30]. Thus, the measured variation in NSC stores across trees is due to changes in carbon supply and other sink demands. Ecosystem models largely treat NSC reserve formation as this *passive* process (reviewed in[30]). Alternatively, the active model of storage posits that NSCs is a sink in itself and carbon may be allocated to reserves at the expense of other sinks[11,13,30,32]. This active allocation may serve as a bet-hedging strategy in stochastic environments and thus assumes that genetic variation in carbon storage measured across trees is due to a genetically regulated tradeoff between carbon storage and other carbon uses, such as growth and reproduction. Accommodating a scenario of active NSC allocation will alter climate model predictions. Specifically, estimates of carbon sink residence times (i.e. biomass, stores, exudates, etc.) and future tree mortality under climate change would be drastically altered, changing our predictions of the length of time and degree to which forests may continue to serve as global carbon sinks.

Differentiating between active versus passive reserve formation has been exceedingly difficult due to the limitations of experimenting on long-lived, slow growing organisms and technical difficulty in extracting and measuring carbohydrates stored in wood. Previous studies have measured

correlations (or lack thereof) between variability in NSC stores and environmental clines or induced stress as evidence for or against active storage[36-38]. However, interpretation of results from these studies is ambiguous and conclusions have been equivocal (eg.[11,32], Figure 1). Here we synthesize previous discussions on this topic[13,15] by proposing-a framework for empirically assessing whether NSC storage is active or passive. We define an *active* process of carbon storage as variation in NSC stores that are (1) under genetic control and (2) tradeoff with other carbon sinks, such that higher storage is favored at the expense of other sinks under certain environmental conditions[13]. Passive NSC storage is indicated by a lack of genetic variation in storage or a lack of tradeoffs with other carbon sinks. Our definition is mechanism agnostic, meaning that active reserve accumulation could be the result of an upregulation of sugar accumulation in cells or a down-regulation in growth or other carbon sinks, previously referred to as "quasi-active storage"[11,30]. We argue that regardless of mechanism, both scenarios represent an evolved, gene-regulated tradeoff which results in the accumulation of sugars and is distinct from the current paradigm of passive NSC reserve formation.

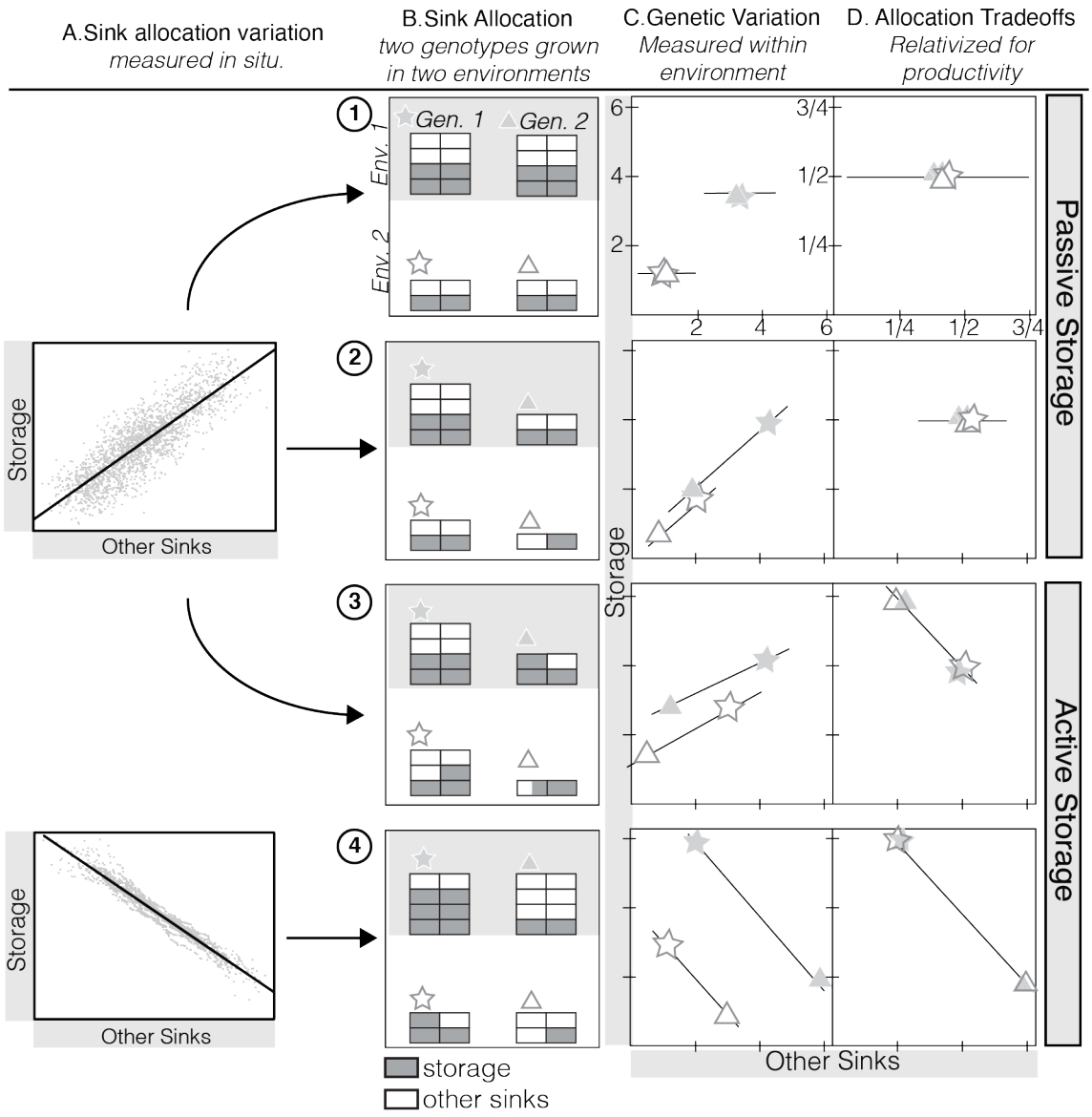

Figure 2.1. For nonstructural carbohydrate (NSC) reserve formation to be considered an active process, NSC storage accumulation must exhibit (1) genetic variation and (2) NSC stores must tradeoff of with other carbon sinks (negative correlation in variance). Here we demonstrate how (A) relationships between carbon sink values measured in the field may be (B) formed in a number of different ways, thus complicating our ability to draw conclusions about active versus passive storage unless both (C) genetic variation is measured and (D) relativized for differences in individual productivity.

Our two criteria for distinguishing active storage are often difficult to assess in practice because carbon sinks are positively correlated with carbon supply and overall tree vigor, referred to here as "productivity". Trees that are more productive have more energy to allocate to growth *and*

storage *and* defense than trees that are less productive[39-41](Figure 1). As such, uncovering allocation tradeoffs is challenging as high variation in productivity can mask variation in allocation strategies (Figure 1, scenario 3). This is best summarized by the analogy of the tradeoff between buying a nice car and a nice house. We know intuitively that individuals must choose how much wealth to allocate to each, and thus a tradeoff exists. However, when examined across all individuals, there is often a positive correlation between nice cars and nice houses, because people with more money can afford better of both (from[39]). Thus, to understand tradeoffs in this context we must normalize by income and to understand tradeoffs in the context of plants, we must normalize by total productivity (Figure 1D).

Decades of common garden experiments have demonstrated that plant productivity varies plastically (between environments) and often genetically (within environments) (reviewed in [42]). Thus, both plastic and genetic variation in productivity have likely complicated previous attempts to identify active versus passive storage from NSC measures taken in the field (Figure 1). Under most conditions, variation measured in NSCs will be positively correlated with variation in other carbon sinks as each sink is also correlated with productivity. Positive correlation amongst sinks could be due to passive mechanisms of carbon storage if there is no genetic variation in NSC storage or plant productivity (all variation is plastic – scenario 1 Figure 1), or if there is genetic variation and plasticity in productivity but not in NSC storage (scenario 2 figure 1). However, this positive correlation could also be the result of active storage if both NSC stores and productivity exhibit genetic variation (scenario 3 Figure 1). Thus, controlling for productivity reveals the genetically determined allocation strategy of each individual. Only under the seemingly unrealistic scenario that productivity is not correlated with carbon sinks will field-measured variation in NSCs show a negative correlation, or trade off, with other carbon sinks (scenario 4).

Here we demonstrate how to test if NSC storage formation is an active or passive process. We quantify genetic variation in carbon productivity, storage, and sinks by measuring traits within a Department of Energy (DOE) common garden of 900+ unique black cottonwood (*Populus trichocarpa*) genotypes replicated clonally 3x each, with full genomic sequences available (Figure S1)[43]. We used direct and indirect measurements of productivity (growing season length), growth (tree volume and relative growth rate), defense (*Venturia* resistance), and storage (root and stem NSC concentrations) traits to test for tradeoffs.

We find strong evidence of active NSC storage in black cottonwood trees. There is ample genetic variation in carbon sinks (including storage) (H^2 = 0.32-0.79, Table S1) and tradeoffs between NSC storage concentrations and other carbon sinks are revealed after productivity is accounted for (sensu Figure 1, scenario 3). As predicted, most carbon related traits (productivity, storage and other sinks) are positively correlated (12/15, Figure 2). Thus, we first used a principle components analysis (PCA) to determine if allocation tradeoffs are masked by large differences in productivity across genotypes (Figure 3). We found nearly half the variation in our data is due to variation in plant productivity as indicated by a gradient of low to high productivity along PC1 (Variation Explained = 41.5%, Figure 3 ABC). PC2, which is formed from the residuals of PC1, then showed a tradeoff between NSC storage and other carbon allocation traits (Figure 3BD). We can further demonstrate this underlying trade off by regressing variance in productivity (represented by PC1) out of our trait values, removing the effect of productivity from each trait, and then correlating the residual sink variance pair-wise (Figure 4). In doing so, we see relationships between sinks flip from positive (Figure 2) to negative (Figure 4). When we relativize our trait data for differences in overall plant productivity, we see allocation tradeoffs emerge. Thus, we demonstrate that genetic variation in NSC storage trades off with genetic variation in other carbon sinks, satisfying the requirement for active storage.

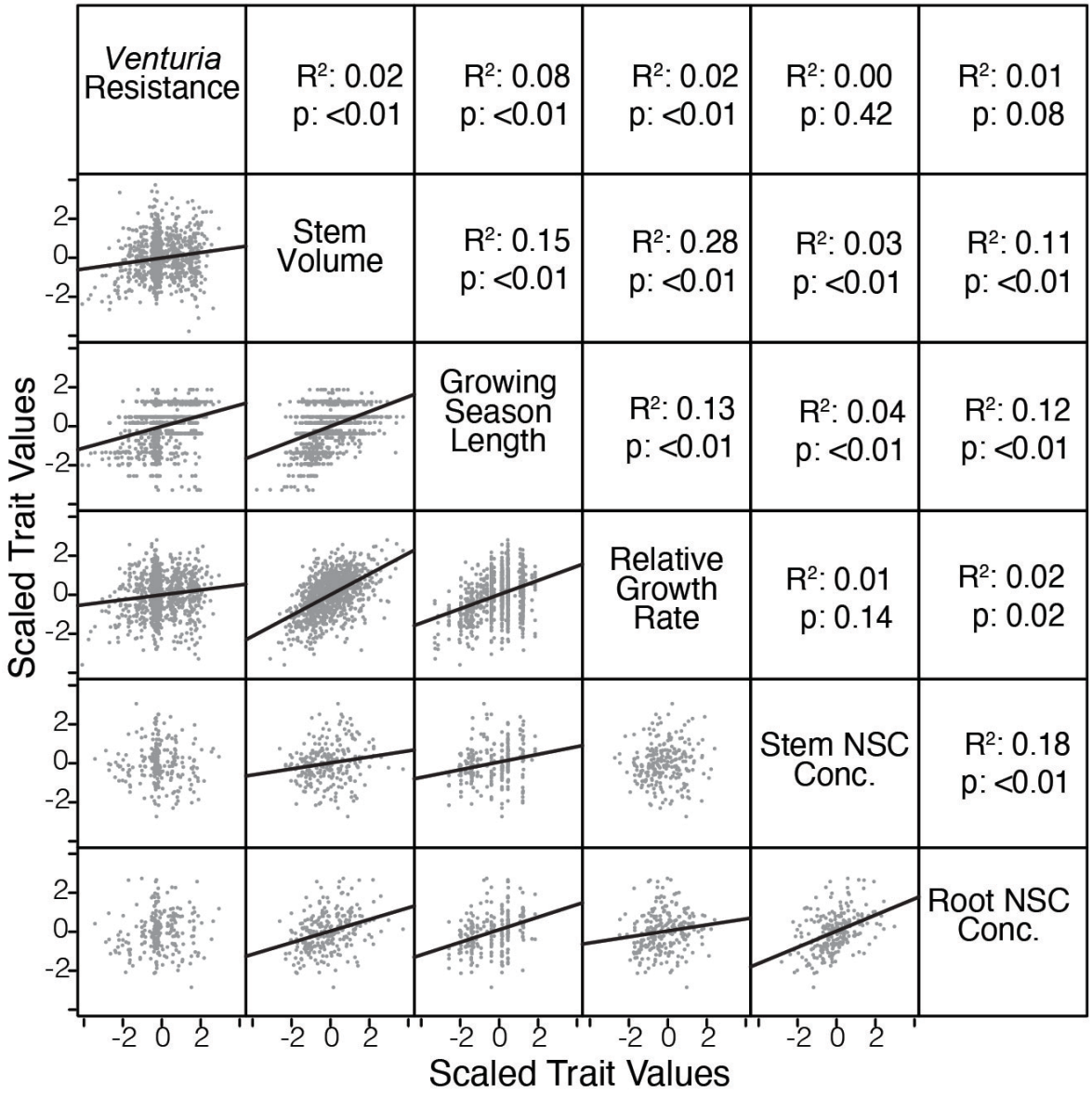

Figure 2. A pairwise comparison of total variation (field measured) of productivity, growth, defense, and storage traits. Trait values are z-scored, with mean centered on zero. We tested for relationships amongst traits via linear regression; all test results are displayed in the top right of the matrix and significant relationships are demonstrated via a fit line in the bottom left.

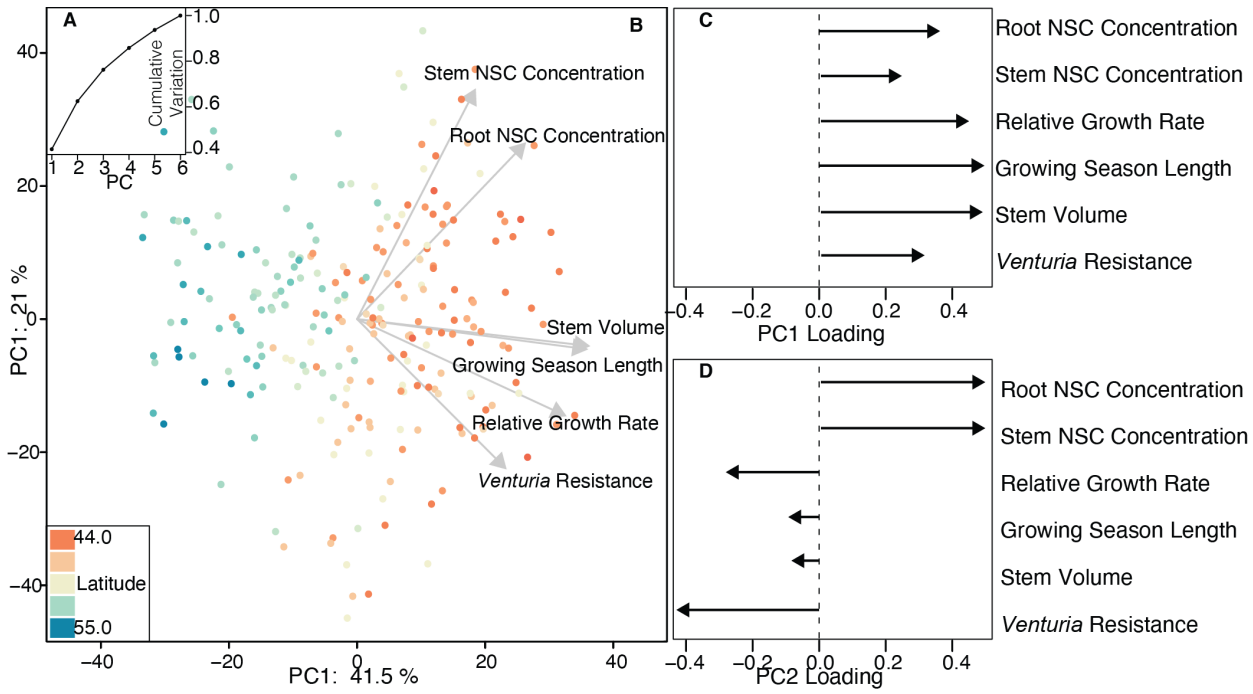

Figure 3. A principle components analysis (PCA) of productivity, growth, defense and storage traits (N = 237 Genotypes). (A) The cumulative variation explained by each PC. (B) The PCA results, where each dot is a genotype in the common garden, colored by the latitude of its provenance, and arrows indicate increasing values of each trait. Each PC is then decomposed in (C) and (D), further highlighting synergies and tradeoffs amongst traits on each PC axis.

Our results demonstrate not only that NSC storage accumulation is an active process, but that there is substantial heritable variation in the degree to which trees invest in storage versus growth and defense within populations (Figure S2), although it is not currently locally adapted. The genetic variation we uncovered is biologically meaningful, as individuals who invest less in growth and defense can store up to 8-10 mg/g, or ~30%, more NSCs in their tissues than their high-growth counterparts (Figure 4). This increased storage capacity may be critical for trees living in temporally or microenvironmentally heterogenous environments (eg.[44]). Given genetic variation provides the raw material on which selection can act, we have demonstrated there is a wide diversity of carbon allocation strategies that are maintained within populations for novel future climate regimes to select

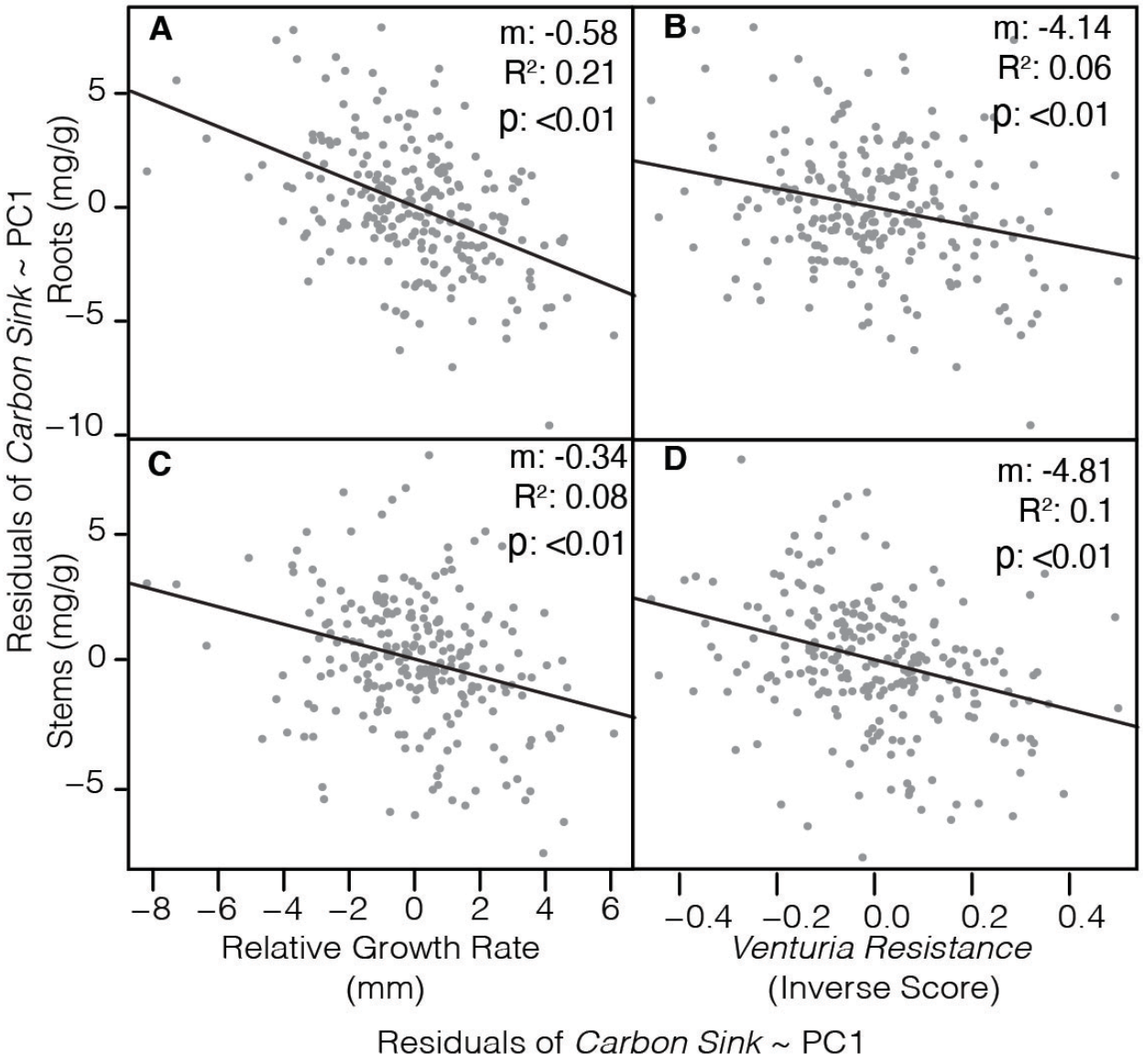

Figure 4. Residuals from linear regressions between genetic variation in growth, defense, and storage (unscaled data) and PC1, which represents differences in productivity between individuals (Figure S7). With variation due to PC1, or productivity, removed the pairwise relationships between carbon sink traits flip from positive, as shown in Figure 2, to negative correlations, indicating a tradeoff hidden by high variation in tree productivity.
on[45].

In conclusion, using common garden trait measurements and building off previous work[33], we were able to demonstrate that NSC reserve formation satisfies the requirements for active storage; it is both (1) under genetic control and (2) exhibits tradeoffs with other carbon sinks. This finding has implications for how we conceptually understand tree physiology and subsequently how

we structure process-based carbon models. With a few exceptions[eg.46], most ecosystem models treat NSC storage as a passive process in which the only way for storage pools to change is if supply or sink demands shift. However, we have demonstrated that NSC reserve formation is at least partially independent of carbon supply and other sink demands. Thus, while models may match past trends, future projections are likely based on flawed assumptions which may be challenged by novel climate regimes.

Methods

To test that NSC storage is an active allocation process, we utilized data collected from a Department of Energy (DOE) common garden of black cottonwood (*Populus trichocarpa*) in eastern Oregon between 2012 and 2017. We used direct and indirect measurements of carbon supply (bud flush/set), structural investment (growth/density), defense (*Venturia* incidence), and storage (root and stem NSC concentrations) traits.

Field Collection

All data were collected from a DOE black cottonwood (*Populus trichocarpa*) common garden, located near Clatskanie, Oregon (46.12°N, 123.27°W). The garden contains three randomized blocks of replicated genotypes along an East-West axis, each containing 917 unique genotypes for a total of 2,751 individuals in the garden. All trees originate from 18 different provenances (referred to here as populations) (Figure 2). Population assignments were taken from a previous publication, where they were generated using sequence data[28]. The collection of each accession is described in Slavov et al.[43] All individuals were planted in 2009 and one replicate was coppiced in December of 2013. All traits were measured prior to this coppicing event except NSC storage. Thus, we have three replicates of uncoppiced trees for all traits, except NSC storage, where we use only the two uncoppiced replicates in our analysis.

Collection of carbon allocation trait data

We chose variables that were direct measures of carbon supply, or a demand pool (defense, growth/structural, storage), or a close proxy. Of the 917 genotypes in the garden, 237 genotypes have replicated measures for all our variables of interest. All individuals in the garden have not yet reached a reproductive age (ie. not yet produced seed or pollen), thus allocation to reproductive traits was not included in this study.

Growing Season Length

We approximated productivity (carbon supply) as growing season length using bud flush and bud set score data that were collected during the 2010 growing season. Earlier bud flush and later bud set correspond to a longer growing season, and thus a larger carbon supply relative to other individuals with later bud flush and earlier bud set in the garden[47]. Phenological timing is locally adapted with early bud flush constrained by selection from frost damage to sensitive leaf tissues, while longer growing seasons are selectively advantageous due to greater resource aquisition[48]. Bud flush scores were taken on March 10 and March 29th, 2010 and bud set scores were taken on September 2nd & 15th, and October 1st, 2010 across all three replicates in the garden. Scores followed previously established criteria (Table S2 & S3) [49].

However, since bud flush and set data were scores and not the actual date of leaf-out and leaf-drop, we used statistical models to estimate the actual start and end dates to the growing season. To estimate the date of bud flush, we combined data from our common garden in Clatskanie, OR with previously published data from a nearby common garden in Corvallis, OR to increase our sample size[28]. We then used the combined dataset to build a logistical regression model, which predicts that probability that a tree has leafed out (ie. is a 1) given the growing degree day (GDD) value and latitude of origin of the genotype. Growing degree data was calculated as the sum of the average daily temperature minus 5^{o}C (representing the minimum threshold for plant growth) and

climate data were taken from daymet[50]. The phenophase data are in stages 0-6, where 0 is a tightly closed bud and 3 represents the beginning of budburst. Thus, we set all observations that were less than 3 to 0 (meaning no bud burst) and observations of 3 or more to 1 (meaning leafout has initiated) for the logistic regression. We then predicted the date where there was the probability of budburst exceeded 50% as the date of leafout using our logistic model (Figure S3).

To estimate the end date of the growing season, we first needed to estimate the actual date of budset from our score data, then estimate the date of leaf-drop given our predicted budset date, since budset occurs when there are still leaves photosynthesizing on trees. To do so, we combined our 2010 budset score information with data on actual budset and leaf-drop dates taken between 2008 and 2010 from the same genotypes, but gown in a common garden in Vancouver, Canada[26]. We got from bud set score to leaf drop date in three stages. The first was to create a logistic regression similar to bud flush using GDD and latitude as predictors and bud set converted to a 0/1 variable, where an observation of 3 or higher was set to 1 and all else 0. Using this model, we then predicted the date on which there was a 50% probability of bud set for each genotype in our analysis. Next, we created a model of the relationship between bud set and leaf drop dates in the Vancouver garden, which contains the same genotypes, but is the only site where leaf drop was measured (Figure S4). This was done using a simple linear regression predicting leaf drop by bud set. Finally, we used this model to predict leaf drop using our estimated bud set dates as the predictor.

Our process resulted in estimates for the start (leaf-out) and end (leaf-drop) date of each genotype's growing season. The purpose of extrapolating from bud flush and set scores to growing season length was to make graphs and discussion more interpretable. To confirm this approach did not bias our results, we reran all analysis using the bud flush and latest bud set scores in our database, finding there to be no change in outcomes (Figure S5).

Disease Resistance

Venturia incidence was observed on leaves on May 30th, 2013 and scored on a 0-4 scale according to the degree of the fungus found on leaves (Table S4). This score was then inversed to represent a metric of disease resistance. All three replicates of each of the 917 genotypes were recorded. *Venturia* is a genus of common, native fungal pathogens, which affect black cottonwoods across their range. It appears on leaves as a whitish film and hinders photosynthetic productivity. In order to fight off infection, trees increase secondary metabolite production of tannins. Previous studies have demonstrated that there is a high degree of variation in tannin production amongst genotypes and thus resistance to *Venturia*[51].

Size and Growth

Two measures of growth were used to capture both primary (vertical) and secondary (horizontal) expansion of tree size. Diameter at breast height (DBH) was measured in mm, approximately 1.5 meters from the ground using DBH tape in November of 2013 and 2014. Relative growth rate was subsequently calculated as the difference between the two growth years. Stem volume was calculated in November of 2014, using measurements of the height of the tree, or tallest shoot, in meters and DBH. Stem volume was calculated as $Volume = \pi \frac{d^2}{2} H$, where radius *d* is the DBH and *H* is the height of the tree. We chose to use relative growth rate and volume rather than DBH and height to be consistent with the carbon allocation trait literature. Both metrics were measured on all 917 genotypes. Given that growth metrics were recorded post-winter coppicing, 2/3 of genotypes had two replicates while the remaining 1/3 had three.

NSC Storage

Finally, we measured the amount of nonstructural carbohydrate (NSC) storage in both aboveground (stem) and belowground (root) tissues. NSCs are stored in the living ray and axial parenchyma cells in wood that must be extracted in lab. Wood tissues were sampled between January 6th and January 10th 2017, from 7a.m. and 4 p.m., as described in Blumstein et al[52]. We

extracted total fructose, glucose, sucrose, and starch, as well as other oligosaccharides and glucans following protocols from Chow and Landhäusser[53,54]. We report these carbohydrate concentrations as one combined metric of total nonstructural carbohydrates, representing sugar and starch concentrations together. We recognize that sampling a single time-point has its limitations given that NSC stores can fluctuate over the course of the year[16]. However, we chose to sample during the dormant season while phloem is largely shut-down. We are ultimately concerned about the relative difference amongst genotypes, which should be largely independent of sampling time.

Calculation of genetic variation and heritability

In a common garden design, we assume that any differences measured between individuals should be the result of genetic differentiation because all individuals are grown under the same climate and site conditions. However, within a garden there may still be microenvironmental variation which causes samples to be spatially autocorrelated (ie. plants growing closer together may be more similar) and vary depending on where in the site they are grown. We corrected for spatial autocorrelation and measured replicate genotypes across randomized blocks to ensure we captured genetic and not environmentally dependent variation. For this process, we conducted all statistical analyses in *R* v.3.5.1 (R Development Core Team, 2018).

To control for spatial autocorrelation in the common garden, we used a thin-plate spline method[28,33] via the *fields* (9.6) package to fit a 3-d surface over values in the garden. We then took the residuals from this surface and used them as our phenotypic estimates.

Using our corrected phenotypic estimates, we parsed genetic variation from the total phenotypic variation measured across replicates. The model followed the formulation

$$(1)\ Y_{ig} = \alpha_g + \varepsilon_{ig};$$

where α is the random effect of each *g* genotype and ε is the residual error of the i^{th} individual of genotype *g*. In the case of our common garden design, the residual error ε represents the deviation

of replicate i from α_g, α_g is the model fit intercept for genotype g, and Y_{ig} is the phenotypic value measured for replicate i of genotype g. We use the α_g estimates for each trait as our measure of genetic variation. For the genotypes that are missing a complete set of three replicates due to coppicing, we expect genetic variation estimates to be pulled toward the grand mean of the model.

To run the model, we used a Bayesian hierarchical model framework, via the *rstan* v.2.18.2 package. All data was modeled as either a normal distribution or a gamma distribution with log link if the data were right skewed (eg. stem volume). The random effect of each genotype (α_g) of equation (1) was estimated using 6,000 random draws from the posterior distribution of the model. We then used the mean value of the draws as our parameter estimate for each trait and genotype. These estimates for the genetic variation in each trait are also known as the best linear unbiased predictions (BLUPs).

Heritability was calculated using the variation parsed from equation (1), following the equation:

$$(2)\ \frac{\sigma^2_{Genotype}}{\left(\sigma^2_{Genotype} + \sigma^2_{Microenvironment}\right)}$$

; where $\sigma^2_{Genotype}$ is the variation due to a tree's genotype and $\sigma^2_{Microenvironment}$ is the residual variation of the model, presumed to be the microenvironmental differences among replicates within a genotype. In the context of our study, $\sigma^2_{Genotype}$ is the variance among α_g's.

Detecting NSC storage tradeoffs

We first compared genetic variation in all traits pairwise via linear regressions, using the base R function "lm". We then used the *vegan* 2.5-5 package in R to examine all traits together in a principle components analysis (Figure 1,S6). Finally, to demonstrate whether tradeoffs arise once productivity is accounted for, we regressed productivity out of sink data and compared the residuals of these models. To do so, we defined productivity as the genotypic values of PC1 from our previous

analysis.PC1 is strongly correlated with growing season length and tree height, both of which are good proxies of higher carbon supply and productivity. We then regressed variation in relative growth rate, stem and root storage concentrations, and Venturia incidence against PC1. We finally compared the residuals of these three models against each other via regression to understand how trait relationships changed once differences in productivity were removed. All models were run using "lm" from the base R environment.

Testing for Signatures of Local adaptation

We used two different metrics to test whether our tradeoff axes exhibited signatures of local adaptation, Q_{st}/F_{st} comparisons and a Qpc test[55]. To calculate a traditional Q_{st} value for our PCs, we determined the degree to which phenotypic variation could be explained by between-population differences versus within-population differences. If populations are locally adapted and a trait is differentially selected across an environmental gradient, then phenotypic variation should be greater between populations and smaller within. To get between and within population variation, we again parsed phenotypic variation using a Bayesian hierarchical model in the package *rstanarm* v.2.18.2. Similar to the model for heritability, the formula includes an extra random effect term for population (α_p):

$$(3)\ Y_{igp} = \alpha_p + \alpha_{gp} + \varepsilon_{igp}$$

We then used the variation due to population (α_p) and the variation due to genotype (α_{gp}) to calculate Q_{st}, or the degree of divergence in a trait's variation among populations versus within.

$$\frac{(4)\sigma^2_{Population}}{\left(2\sigma^2_{Genotype} + \sigma^2_{Population}\right)}$$

We use the equation from Whitlock and Gilbert[56], which includes a 2 in the denominator due to the additional nested variable in the model. If variation among populations is higher than variation

within populations, our results are consistent with directional selection across populations. We can further compare whether the value of Q_{st} is representative of selection or random processes by comparing it to F_{st}, or the variation at neutral genomic loci between and within populations. Traits varying due to selection across the environment are expected to have Q_{st} exceeding neutral variation in F_{st}. F_{st} estimates were taken from previous work[28], where F_{st} was calculated in 1-kb windows using all 917 genotypes available in the mapping population as $(\pi_T-\pi_S)/\pi_T$; where π_T is SNP diversity across all individuals and π_S is weighted within-population SNP diversity[28].

3

Adaptive variation and plasticity in nonstructural carbohydrate storage concentrations in a temperate tree species

In submission as:
M. Blumstein & R. Hopkins. *In submission*. Adaptive variation and plasticity in nonstructural carbohydrate storage concentrations in a temperate tree species.

Summary

1. Trees' *total* amount of nonstructural carbohydrate (NSC) stores and the *proportion* of these stores residing as insoluble starch are vital traits for individuals living in variable environments. Given projected climate change, it is crucial to understand the plastic and evolutionary potential of such critical traits to predict species' potential for survival.
2. Here, we measured the amount of environmental and genetic variation in these traits using branch samples taken from black cottonwood (*Populus trichocarpa)* trees grown in two common gardens.
3. We found heritable variation in both total NSC stores and the proportion of stores in starch (H^2_{TNC} = 0.19, $H^2_{PropStarch}$ = 0.31), but no signatures of current local adaptation (Q_{st} <= F_{st}). In addition, we found high amounts of plasticity in both traits, with most plastic variation in the proportion of NSC stores in starch due to environment (97%), while the plastic variation in total NSC stores is largely attributable to genotype-by-environment interactions (54%).
4. Overall, we found total NSC concentrations and the proportion of NSC in starch have both adaptive genetic variation and plasticity, enabling these traits to bolster forest tree species against climate change over the short-and-long term.

Introduction

Climate is changing and extreme temperature and precipitation events are expected to intensify over the coming century [57], presenting immense challenges for immobile, long-lived organisms such as trees. Rates of forest tree mortality are already increasing worldwide as a result of shifting drought regimes, extreme temperatures, and pest outbreaks associated with global change [3,58-60]. In response to change, individual plants may physiologically adjust by plastically altering traits in the short term [61-66], while populations may undergo local adaptive evolution through shifts in their genetic composition over longer time scales [67,68]. Thus, understanding the extent to which trees are able to

alter their traits in response to climatic change over short (plastic) and long (evolutionary) timescales is critical to predicting species' survival.

One key trait that enables plants to tolerate stochastic environments is the storage of nonstructural carbohydrates (NSCs). NSCs are the sugars and starches produced via photosynthesis and stored in the parenchyma cells of plants' woody tissues for later use [13,14]. NSCs fuel photosynthesis at night, leaf-out in spring, and are also thought to serve as a back-up osmolytic or energetic reserve during periods of environmental extremes, like drought or freezing temperatures [9,13,36,37,69]. Total NSC storage concentrations are known to vary seasonally eg. [16], across species eg. [70], and within species eg. [33] and this variation in NSC storage concentrations has been linked to prolong survival under drought [34]. However, what controls variation in total NSC stores and how sensitive it is to environment is still poorly understood. Thus, we are limited in our ability to predict whether forest trees will be able to vary NSC stores in order to tolerate or adaptively evolve in response to climate change.

Total NSC stores can be broken down into two categories: soluble sugars and insoluble starches [71-73]. Sugars affect cells' osmotic balances and are readily accessible for metabolism as they are dissolved in solution, while starches are considered the longer-term storage molecule as they are insoluble and thus must be broken back down into sugar to be used by the cell as an osmolyte or metabolite. Sugars can hydrolyze into and out of starch form via a number of enzymatic pathways [73]. The rate of starch transition varies daily [74], seasonally [16,19,70,75], by plant tissue [16,70], and in response to stress, such as water deficit [36,37,76,77], high salinity [78-82], or extreme temperatures [83-86]. Under such environmental stressors, starch is degraded, leading to a subsequent rise in soluble sugars in stressed tissues [73] and an increased ability to withstand the applied stress. Thus, a plant's ability to convert NSC stores from starch to sugar, and back again, is an important consideration for survival under climate change. While variation in starch degradation rates in response to environment is well

document, it is not yet understood if individuals exhibit differential sensitivities to environment, indicating a potential for adaptive evolution in response to increased stress.

Given that both the *total* amount of NSC stores a plant holds and the *proportion* of those stores reserved in starch can play crucial roles in woody plant survival under environmentally induced stress, measuring the degree of heritable genetic and plastic variation in these traits will be critical for predicting tree species' persistence under climate change. Transplant experiments across multiple sites with replicate clones or related individuals can be used to disentangle sources of variation [55,87]. Genetic variation in these designs is measured within an environment across unique genotypes, while plastic variation is measured across environments within unique genotypes. In practice, because measuring plastic variation results in the additional capture of genetic variation by virtue of gathering data from multiple common environments, it is often broken down into three components; variation *within* a garden attributed to genetic differences (G), variation *between* gardens attributed to environmental plasticity (E), and the interaction between genotype and environment (GxE) (ie. some genotypes can be more plastic than others). While there is strong evidence that heritable genetic variation is responsible for some of the variation in NSCs in some plants such as *Populus trichocarpa* [33] and *Pinus sylvestris* [88], to our knowledge, no study to date has quantified the extent of plastic variation in NSCs. Furthermore, no study has examined genetic or plastic variation in the proportion of NSC that is kept in starch versus sugar, a potentially critical aspect of plant response to stress.

By partitioning the variation in NSCs we can not only predict the potential for tress to respond to increased prevalence of stress, we can also begin to understand if trees are already locally adapted to variation in environmental stress across their ranges. If greater total NSC storage and more rapid transition between starch and sugar storage can increase survival in stressful events, we predict genetic variation in these traits to reflect geographic variation in stress. By controlling for

neutral population genetic variation across the range of a tree species (*e.g.* Fst) we can determine the extent to which traits show genetic differentiation (e.g. Qst) reflective of local adaption.

Here, we measure genetic and plastic variation in *total* NSC storage and the *proportion* of NSC stores held in insoluble starch versus soluble sugars. To do so, we utilized two Department of Energy (DOE) common gardens of black cottonwood (*Populus trichocarpa*) growing in the western United States. Each garden contains clonally replicated genotypes from multiple populations across the species range. We extracted sugars and starches from branch woody tissue of trees grown in two common gardens located at similar latitudes, but spanning a continental to coastal environmental cline (Figures 1 & 2A). Our objective is to understand the acclimatory and evolutionary potential of black cottonwood trees under future climate change. We accomplish this by parsing the amount of phenotypic variation attributable to genetic variation (G), environmental plasticity (E), and genotype-by-environment interactions (GxE) for both the total concentration of NSC stores, as well as the proportion of total stores in insoluble starch. In addition, we search for signatures of current local adaptation in both traits across the environmental gradient of source populations.

Materials and Methods

Sample collection

We collected branch samples from two Department of Energy (DOE) common gardens in Oregon, USA in January of 2017. The gardens are located near Clatskanie, Oregon (46.12°N, 123.27°W; MAT = 10.4ºC, MAP = 1,545 mm) and Corvallis, Oregon (44.56°N, 123.26°W; MAT = 11.2ºC, MAP = 1,030 mm) respectively, which represent contrasting environments with similar daylength patterns (Figure 2A). Each garden contains the same 1,060 unique genotypes from 19 populations, which were replicated clonally three times each and planted out in 2009. The collection of each accession is described in Slavov et al. [43]. However, we only sampled genotypes from 17 of the

populations, as some populations had high mortality, and from the 917 of 1,060 which have full genomic information available[28] (Figure 1). In Corvallis, all three replicates were coppiced (aboveground biomass harvested) in the winter of 2013-2014, while only one replicate was coppiced in Clatskanie during the same period (Figure 1). Thus, we only sampled branches from coppiced replicates for this study. Non-coppiced trees in Clatskanie had an average diameter at breast height (DBH) in 2016 of 155.2 ± 46.9 mm, while coppiced trees averaged 84.0 ± 28.0 mm. DBH in Corvallis across all coppiced replicates in 2016 was 44.4 ± 14.9 mm.

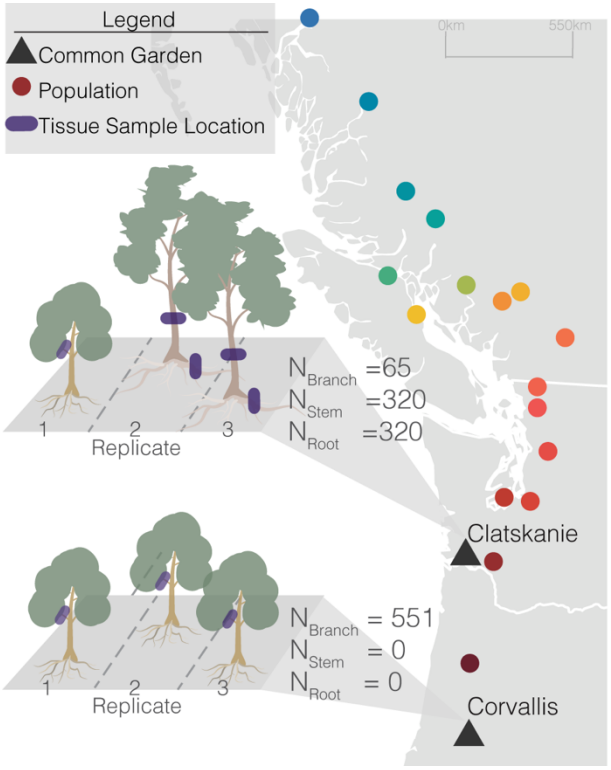

Figure 1. The transplant design. Genotypes were sourced from 17 populations from across western North America and replicated three times each in two common gardens located in Clatskanie and Corvallis. In the winter of 2013-2014, one replicate in Clatskanie and all three replicates in Corvallis were coppiced aboveground and allowed to regrow (shown as small trees). Sample tissues collected in January 2017 are reflected by the purple ovals with the subsequent number of samples taken of each tissue from each garden indicated.

We collected all samples between January 6th and January 11th 2017, between 7 A.M. and 4 P.M. using pruning shears for branch sampling. We took All branch samples as 2cm segments from

the previous growing season's growth segment (2015) of coppiced replicates as it was accessible across all individuals. All samples were kept on dry ice during field collection, then shipped overnight to Cambridge, MA and stored at -80^{O}C. In total, we collected and processed 616 branch samples (Figure 1).

We collected additional stem and root tissue during this time period. Their collection and total nonstructural carbohydrate concentrations are reported in a previous publication [33]. However, because only total NSC stores for these samples are previously detailed, we include heritability estimates for sugar and starch separately in the supplement of this paper for comparison (Table S1).

NSC Laboratory Preparation

We initially freeze-dried samples for 24-hours (FreeZone 2.5; Labconco, Kansas City, MO, and Hybrid Vacuum Pump, Vacuubrand, Wertheim, Germany), then ground them to a fine powder (mesh 10, Thomas Scientific Wiley Mill, Swedesboro, NJ, USA; SPEX SamplePrep 1600; MiniG, Metuchen, NJ) and stored them in sealed glass vials. Sugar and starch extraction protocols were adapted from Chow & Landhäusser [53].

We extracted sugar from 20 mg of dried, ground tissue using 80% hot ethanol, followed by a colorimetric assay with phenol and sulfuric acid, and read using a spectrophotometer at 490nm (Thermo Fisher Scientific GENESYS 10S UV-Vis, Waltham, MA). We calculated sugar concentrations of mg sugar per g of dry wood using a 1:1:1 glucose-fructose-galactose standard curve (Sigma Chemicals, St. Louis, MO). We extracted starch using the tissue remaining after sugar extraction. We solubilized tissue in NAOH, then incubated it for 24-hours with alpha-amylase and amyloglucosidase digestive enzymes, which digested starch into glucose. We then assayed the solutions using a PGO-color reagent solution (Sigma chemicals) and read them on the

spectrophotometer at 525nm. Starch concentrations of mg glucose-starch-equivalent per g dry wood were calculated based on a glucose standard curve (Sigma Chemicals).

For all lab analyses, we included at least two internal laboratory standards (*Quercus rubra* stemwood from Harvard Forest, MA; 42.01 ± 5.13 mg•g-1 Sugar, 30.17 ± 4.23 mg•g-1 starch). This acid methodology extracts all fructose, glucose, sucrose, and starch, as well as other oligosaccharides and other glucans [54]. We then report these metrics as *sugar* and *starch* concentrations (mg•g-1) in the supplement, as well as the *total nonstructural carbohydrates (TNC)* concentration (sugar + starch) and the *proportion* of starch to total (starch/ (sugar + starch)) in the main text. All statistical analyses were performed in *R* v.3.5.1[89].

Determining environmental conditions of population origins and gardens

We accessed Daymet daily meteorological data for the past 38 years (1980-2018) at each site via the *daymetr* package in R[90]. Daymet data are 1km^2 gridded estimates of daily weather variables, interpolated from weather station data[50]. Using these data, we calculated common descriptive climate variables that represent the temperature and aridity of our genotype provenances and 2 common garden sites. All climatic variables we calculated were highly colinear, thus we used a PCA analysis to describe the major axes of variation via the *vegan* v.2.5-3 package in R [91] (Figure 2A).

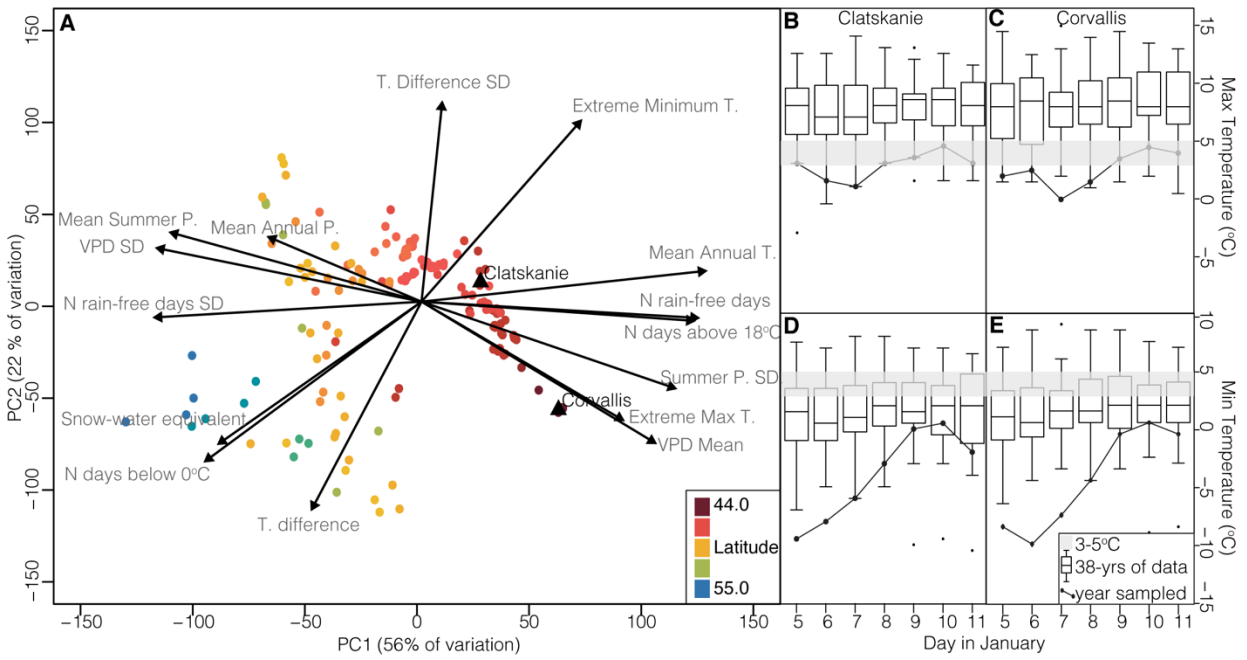

Figure 2. (A) A principle components analysis (PCA) of the climate over the past 38 years at each of the genotype's source locations and the two common gardens. Dots represent each genotype's source location in climate space, colored by latitude, and the two black triangles represent the common gardens in the climate space. (B-E) The average minimum and maximum temperatures over the past 38 years in Clatskanie and Corvallis (boxplots) as compared to the minimum and maximum temperatures in the year we collected samples (2017, black lines). Samples were collected in (B,D) Clatskanie on January 5th – January 9th and in (C,E) Corvallis on January 10th- January 11th. Data is sourced from Daymet [50].

Control for spatial autocorrelation

In common garden studies the spatial autocorrelation, or the probability that individuals growing closer together are more similar, of samples must be taken into account [92]. To account for geographic patterns within each of our gardens (Clatskanie and Corvallis), we used a thin-plate spline method [28,33]via the *fields* (9.6) [93] package in *R*. This method fits an interpolated surface to the garden, which uncovers regions of each site that significantly differ from the mean. To correct these patterns of spatial concordance, we take the residuals from the thin plate spline and add them back to the model intercept, thus removing spatial trends and placing sample values back on a biologically

meaningful scale. We did this for each of our metrics independently; sugar concentration, starch concentration, total nonstructural carbohydrate (TNC) concentration, the proportion of starch (starch / TNC), and diameter at breast height (DBH).

Calculating the genetic contribution via heritable variation

We estimated components of variation across all the data from both gardens to calculate broad-sense heritability and Q_{st}. The spatial autocorrelation corrected data were used to parse variation in our nested hierarchical structure of population, genotype, and environment via the following equations:

$$(1) Y_{Gigp} = \ ß_G + \alpha_G + \ \alpha_{Gp} + \ \alpha_{Gpg} + \varepsilon_{Gipg}$$

Our goal is to quantify within-garden genetic variation, we therefore parsed variation in branches grown in two different gardens (G) using the fixed effect $ß_G$. The parameters *p* for population (i.e. provenance of genotype), g for genotype, and *i* for the i^{th} individual tree sampled are all random effects. All branch data were modeled as gamma distributions using Bayesian mixed regression models via the package *rstan* v.2.18.2 in [94]. The random effects outcomes ($\alpha's$) and fixed effect ($ß_G$) of equation (1) were estimated as the mean of 6,000 random draws from the posterior distribution (Table 1 & S1).

Table 1. Phenotypic means and standard deviations, variance component estimates from equation (1), and parameters for total nonstructural carbohydrate (TNC) storage concentrations and the proportion of total stores in starch of branch tissues of black cottonwood trees.

Branch Trait	Clatskanie		Corvallis								
	μ	σ	μ	σ	(σ^2_{Gipg})	(σ^2_{Gpg})	(σ^2_{Gp})	(σ^2_{G})	(β_G)	H^2	Q_{st}
TNC	30.8	8.3	30.3	6.2	31.39	6.567	1.004	222.759	-0.099	0.19	0.07
Proportion	0.2	0.07	0.1	0.08	0.002	0.001	0	0.003	-0.102	0.31	0.04

The resultant fixed and random effect estimates ($ß_G + \alpha_G + \alpha_{Gp} + \alpha_{Ggp}$) from equation 1 were then used as our genetic estimate for each genotype and are displayed in all graphical analyses (often referred to as a Best Linear Unbiased Prediction or BLUP). The variation parameters estimated from equation 1 were used to calculate broad-sense heritability, H^2, and Q_{st} of each of the traits. H^2 was calculated for all traits in stems, branches, and roots, using the random effects variances from equation (1) as:

$$(2)\ (\sigma^2_{Genotype} + \sigma^2_{Population}) \,/\, (\sigma^2_{Population} + \sigma^2_{Genotype} + \sigma^2_{Microenvironment})$$

Population variance was included with Genotype as it is also representative of genetic differences between individuals. Genotype variance was taken as the variance among replicates and microenvironmental variance was taken as the residual variance of the model. Q_{st} was calculated via the formula [95,96]:

$$(3)\ \sigma^2_{Population} \,/\, (2\sigma^2_{Genotype} + \sigma^2_{Population})$$

F_{st} was taken from a previous publication using the same genotypes and calculated in 1-kb windows as $(\pi_T\text{-}\pi_S)/\pi_T$; where π_T is SNP diversity across all individuals and π_S is weighted within-population SNP diversity [28].

Calculating plasticity: environmental and genotype-by-environment contribution

Plastic variation is defined by Scheiner and Goodnight as the variation due to environment (E) and genotype-by-environment (GxE) interactions [97]. To calculate each, we used a Bayesian mixed model regression analysis in R using the *rstanarm* v. 2.19.2 package[98] via the following equation.

$$(4) Y_{igG} = \alpha_G + \alpha_g + \alpha_{G:g} + \varepsilon_{igG}$$

The model calculates the variation within the random effects of Environment (G or Garden), Genotype (g), and GxE (G:g, or Garden:genotype). We then use these variances, estimated as the

mean of 6,000 random draws from the posterior distribution of equation (4), to calculate the contribution of an individuals' phenotype due to plasticity, also known as the *S* index[99].

$$(5)\ S = (\sigma_E^2 + \sigma_{GxE}^2)/(\sigma_G^2 + \sigma_{GxE}^2 + \sigma_E^2 + \sigma_e^2)$$

We then used these properties to calculate the proportion of plasticity due to environment versus genotype-by-environment interactions (Table 2).

$$(6)\ \sigma_{Plasticity}^2 = (\sigma_E^2 + \sigma_{GxE}^2)$$

We build this model separately from our heritability model because of the way H^2 and S are defined in the literature. Plasticity (S) estimates require us to separate variation due to GxE interactions from genetic variation. However, GxE interactions would be partially captured under the umbrella of genetic variation in our heritability model. Conversely, our heritability model also examines the variation due to population in order to calculate Q_{st}, which is partially captured by the G and GxE random effect terms from our plasticity model. In order to accurately parse the subtle differences in how heritability and plasticity define genetic variation, we run two separate models.

We also used Relative Distance Plasticity Index (RDPI) as a measure of genotypic plasticity, which is a more general way of calculating plasticity that doesn't rely on assumptions of the underlying distribution of the data[63] .

$$(7)\ RDPI = \sum \frac{|X_{Clatskanie} - X_{Corvallis}|}{max(X_{Clatskanie}, X_{Corvallis})} / N$$

RDPI measures the absolute difference in genetic trait values between genotypes grown in two different environments, then normalizes that measure by the maximum of the two values. All of these measures are then summed and divided by the number of samples to get the final average RDPI metric.

Results

Environmental conditions of population origins and gardens

Our genotypes originated from a steep climatic gradient of temperature (mean annual temperature: 10-17°C), aridity (mean annual precipitation: 609mm-2,705mm), and continentality (temperature difference between hottest and coldest month: 14 – 26°C). When summarized via a Principle Components Analysis (PCA), the first major axis of variation amongst climate variables across sites (PC1) describes an axis of cold and wet sites to hot and dry sites (Figure 2A). The second axis of variation represents continentality, ranging from sites with consistently cold winters and high amounts of snowfall to sites that are generally warmer and do not experience as extreme lows (Figure 2A). In comparison to Clatskanie, Corvallis is hotter, drier, and has more continentality, meaning colder, wetter winters and hotter, dryer summers.

While these are the average site conditions, at the time of sampling, both Clatskanie and Corvallis experienced the lowest temperatures recorded for those dates over the past 38 years (Figure 2 B-E, solid line). Minimum temperatures ranged from -10°C to 0°C and maximum temperatures never reached higher than 3-5°C. This is a key detail as starch synthesis and degradation enzymes cease to perform under 3-5°C [100], thus these short-term temperature drops may have influenced our measures (Figure 2 B-E).

Total phenotypic variation

Across all tissues measured, NSC concentrations were highest in branches (Clatskanie: 30.8 ± 8.3 $mg \bullet g^{-1}$, Corvallis: 30.3 ± 6.2 $mg \bullet g^{-1}$) and lowest in stems (Clatskanie: 15.6 ± 6.0 $mg \bullet g^{-1}$) (Table 1 & S1, Figure S1). The proportion of total NSCs in starch ranged from 0.10 ± 0.08 in branches in Corvallis to 0.28 ± 0.18 in roots in Clatskanie (Table 1 & S1, Figure S1).

The genetic contribution (G)

We found heritable variation in branches for both total NSCs and proportion of NSCs in starch (Table 1, Branch $H^2_{TNC} = 0.19$, Branch $H^2_{PropStarch} = 0.31$). As previously reported, this is similar heritability as total NSC storage in *P. trichocarpa* stems and roots Table S1; [33]. Here we found that the proportion of starch to total stores is also heritable in roots (Root $H^2_{PropStarch} = 0.37$), but not stems (Stem $H^2_{PropStarch} = 0.01$).

Branch genetic variation does not exhibit high degrees of across population variation in either total NSCs or proportion of stores in starch ($Q_{st\ TNC} = 0.07$, $Q_{st\ Proportion} = 0.04$; Table 1). This stands in contrast to stems and roots, which demonstrate extensive differentiation across populations in total stores ($Q_{st\ Roots} = 0.30$, $Q_{st\ Stems} = 0.31$) and stem partitioning between sugar and starch ($Q_{st\ Stems} = 0.66$) (Table S1). However, the finding of high Q_{st} value for stems in the partitioning between sugar and starch is unlikely biologically meaningful. H^2 for stems is only 0.01 for this trait, thus the high Q_{st} value is calculated using just 1% of the phenotypic variation measured.

Plasticity: Environmental Contribution (E)

The proportion of NSC that trees put into starch vs. sugar is a plastic trait by both metrics of plasticity, RDPI and *S* (Table 2, $RDPI_{proportion} = 0.50$, $S_{proportion} = 0.74$). This plastic variation is largely attributable to the effect of garden, which explains 97% of total plasticity (equation 7; Table 2, Figure 3). On average, Corvallis has higher sugar concentrations and lower starch concentrations, while Clatskanie has higher starch concentrations and lower sugar concentrations (Figures 3B & S2, Table 1). This pattern is reflected in the proportion of NSC stores in starch, where the proportion of starch to total stores in Corvallis is 50% more than in Clatskanie (Figure 3B). Thus, there is a clear difference in the degree to which total stores are partitioned between sugar and starch within each garden.

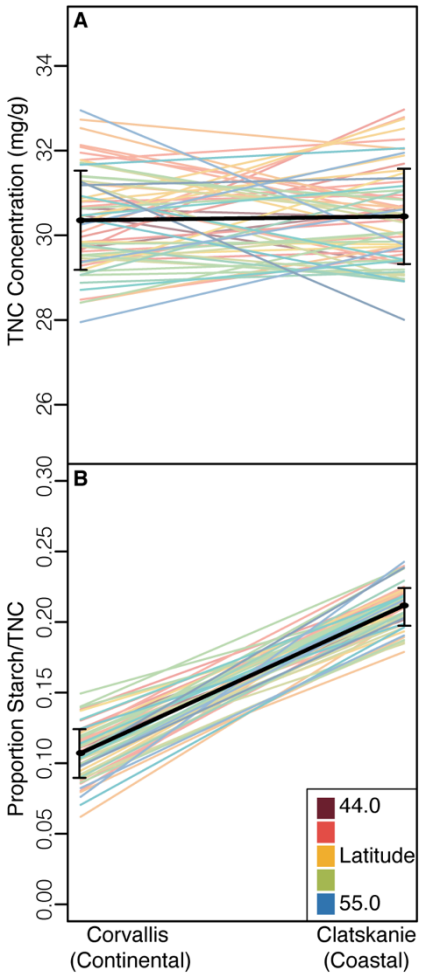

Figure 3. Plasticity between the two common gardens in the two traits measured, (A) total NSC stores (TNC) and (B) the proportion of TNC in starch. Black lines represent the average value across all genotypes, with error bars indicating one standard deviation from the mean. The other lines are colored by latitude and each line represents a genotype, where genotype values were estimated using equation (1).

Table 2. Variance component estimates from equation (4) and parameters for total nonstructural carbohydrate (TNC) storage concentrations and the proportion of total stores in starch of branch tissues of black cottonwood trees.

Branch Trait	σ^2_g	σ^2_G	$\sigma^2_{G:g}$	RDPI	S	(%) of S that is GxE
TNC	2.4	3.4	3.2	0.03	0.43	46
Proportion	0.025	0.091	0.017	0.5	0.75	3

In contrast, total NSC stores are only considered environmentally plastic by one metric ($RDPI_{TNC}$ = 0.03, S_{TNC} = 0.43). Only 54% of the plastic variation (*S*) measured is explained by environment, while the rest is attributed to GxE effects. Thus, we find high genetic variation in TNC across the gardens, but low plasticity and almost no difference between the two gardens in average total NSC concentrations (Δ_{garden} = 0.5 mg•g-1, Table 1, Figure 3A).

Plasticity: Genotype-by-Environment Contribution (GxE)

Genotype-by-environment interactions explain almost 50% of the variation between gardens in total NSC stores (Table 12 Figure 3A), but only 3% of the variation between gardens in the proportion of NSC in starch (Table 2, Figure 3B). Thus, genetic differences explain most of the variation in total NSC stores, while plasticity explains most of the variation in the proportion of starch vs. sugar.

In addition, some genotypes are more plastic than others, particularly in the amount of NSC they allocate to starch (Table 2, Figure 4). This pattern of increasing plasticity follows a latitudinal trend, where northern populations are more plastic in each trait measured than southern populations (Figure 4). However, while data trend this way, they are not significant at the 0.05 level (Figure 4).

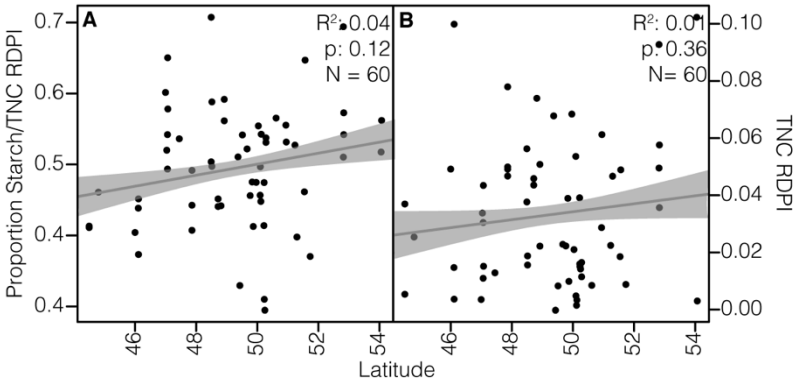

Figure 4. The relative distance plasticity index (RDPI) of the (A) proportion of starch to total and (B) total amount of NSC stores plotted by the latitude of each genotype's source location. Black dots

represent each genotype's RDPI and the line fits are shaded gray for one standard deviation. A larger RDPI indicates that there is a larger percent change in genotypic trait values between gardens.

Discussion

Genetic (G) variation in both total stores and partitioning between sugar and starch

Genetic variation in traits act as the raw material with which populations can adapt to novel stress. Here, we found heritable genetic variation in total NSC concentrations (sugar + starch) in the branches of black cottonwood. Our results reveal that these trees could potentially evolve greater NSC storage in response to increased stress. An increase in the concentration of NSC a tree stores may confer enhanced resilience during times of photosynthetically limiting stress by serving as a fuel source or osmotic reservoir [9,30,32,34,101]. Experimental and observational studies have demonstrated that trees will draw down NSC stores when experiencing photosynthetically limiting environmental conditions [36,37,77,102,103], such as drought, suggesting that NSCs may be serving a critical metabolic function. In addition, seedlings with higher NSC stores live longer through drought, indicating that higher NSC concentrations may enable trees to live longer under environmental stress [34]. Given that climate forecasts generally predict more extreme weather events [5], the existence of heritable variation in total NSC stores may be crucial for tree populations to evolve in response to climate-driven selection in the future.

In addition to total storage, the proportion of stores individuals put into starch versus sugar at any given time may be crucial for withstanding future climate-driven selection. We also found heritable variation in the proportion of these total stores residing in insoluble starch for branches, stems, and roots (Table 1, Table S1). Across most winter deciduous species, the proportion of total stores in starch is at its lowest in the winter, particularly in January, the month we sampled in [16,70]. This is thought to be because the rate of starch degradation and synthesis is controlled in part by enzymes with different temperature sensitivities. Starch degradation enzymes are less sensitive to

low temperatures than starch synthesis enzymes [100], although below 3-5°C both degradation and synthesis enzymes cease to function. Thus, at low temperatures (but still above 3-5°C) starch is degraded, leading to a corresponding increase of sugar in cells [104]. This newly available pool of sugar can be used for maintenance respiration and may confer an increased cold tolerance to individuals or even signal when to break dormancy in spring [105]. Thus, being sensitive to changes in temperature and shifting stores between starch and sugar may be critical for tree survival under future, more chaotic climate regimes. Our results indicate that there is genetic variation in if or how trees shift stores between starch and sugar. This opens the possibility that trees can adapt their allocation strategy to better fit a changing, more stressful climate.

Although we found heritable variation in both branch total NSC stores and proportion of stores in starch, we did not find evidence that this variation was currently locally adapted. Differentiation across populations in genetic variation of these traits is minimal. The lack of adaptive signatures in branch total NSC stores stands in contrast to adaptive differentiation previously reported for stems and roots. One reason for this divergence may be that branches are the most proximal of the three tissues to carbon sources (leaves) and some sinks (buds and flowers). Over the course of a year, branch NSC stores fluctuate much more than roots or stems as they are the first storage sink to fill with new photosynthates and the first to be drawn down in spring [16]. This pattern could also be caused by the fact that black cottonwoods have photosynthetic bark. Branches are exposed to more sunlight than stems and roots and thus may see a higher degree of variation in NSC produced via opportunistic bark photosynthesis. Together, these sources of variation may have a genetic signal, but the other sources of fluctuations may mask the genetic variation in storage preventing selection from effectively causing genetic differentiation.

Environmental (E) plasticity in partitioning between sugar and starch

Immediate response to stress depends on an organism's ability to plastically adjust trait values to accommodate changing environments. The degree to which an organism can plastically respond will, in many causes, determine its ability to survive stress. Here, we found extensive plastic variation due to environmental response in the proportion of NSC stores in starch versus sugar (Table 2, Figure 3, solid black lines). In Clatskanie an average of 20% of total NSC stores were found in starch, while only half that amount was found in Corvallis (Figure 3). Clatskanie has a coastal climate with rainfall spread throughout the year and small temperature differences between winter and summer (Figure 2). In contrast, Corvallis has a continental climate which regularly experiences extreme temperatures and long periods without rainfall (Figure 2). Thus, these results may reflect the differential enzymatic sensitivities of starch degradation and synthesis to average climatic conditions at these two sites [100,105]. The warmer average temperatures in Clatskanie could have led to a higher proportion of NSC being left in starch while the colder, more stressful conditions of Corvallis resulted in more sugar storage.

The observed plasticity in proportion of starch storage could also be driven by the weather patterns on the dates of sampling. We happened to collect woody tissues on the coldest days recorded over the past 38 years in Clatskanie and extremely cold days in Corvallis (Figure 3). Low temperatures in Clatskanie fell below -10°C some days and highs never went above 4°C, within the minimum temperature range that starch synthesis and degradation enzymes can work [100]. The sharp drop in temperatures due to the polar vortex may have halted enzymatic activity entirely. Thus, instead of starch steadily degrading to sugar as temperatures drop, the quick temperature change may have prevented starch from degrading further. Conversely, we travelled to Corvallis after sampling in Clatskanie, where the temperature reached just above 5°C on our sample dates; just above the minimum temperature range for enzymatic activity. Thus, starch may have degraded into

sugar in trees at this site. Such a quick change could be possible given that starch synthesis and degradation have been observed on diurnal scales [74].

It is difficult to pinpoint whether the plasticity in the proportion of NSC in starch between the two gardens was attributable to the average climate of the two sites, or the weather at the time of sampling. However, there is mounting evidence that this plasticity in the synthesis and degradation of starch in plants is critical for seasonal signaling in plants [15,105,106]. Branch NSC stores begin to synthesize from sugar into starch as temperatures rise in spring [16,70], and this process likely occurs faster in branches than in roots because branches are exposed to air and not insulated in the soil. Thus, temperature gradients across the plant may drive the movement of carbohydrates upward in spring to support leaf flush and stem growth [107]. This synthesis of starch or movement of carbohydrates could be the signal plants sense in spring to break dormancy or initiate leafout. Thus, it may be this plasticity in the conversion of sugar to starch that is in part driving observed plasticity in phenological timing, a key trait for future tree adaptation to climate change [108-110].

Environmental plasticity in total NSC stores unveiled when tree size is considered

While partitioning of stores between sugar and starch is plastic, we found total NSC stores to be the same, on average, between the two gardens. This is particularly interesting as the timing of leaf out and growth rates of trees significantly differ between the two sites. In Clatskanie, leaves come out earlier than Corvallis, potentially giving the Clatskanie trees a greater opportunity to produce carbon compared to the Corvallis trees[28]. This carbon advantage is reflected in the diameters of trees at both sites, where trees in Clatskanie are almost double the size of trees in Corvallis (Figure 5). However, both sites average the same total NSC storage concentrations. Without the growth data, total NSC stores appear to have no environmentally driven plasticity, however with the growth data, the lack of difference between the two sites could actually be

indicative of environmental plasticity in a tradeoff between the growth and storage. Trees growing in more variable or extreme conditions may "bet-hedge" by storing more NSC at the expense of other uses, such as growth [11,32]. This particular pattern has been shown in Arabidopsis, where plants favor storage over growth when photosynthetic productivity declines [106,111]. Our results here suggest that this may be similar in the case in black cottonwoods, where genotypes grown in the continental garden (Corvallis), with larger temperature and precipitation extremes, maintain the same concentration of stores, but down-regulate growth to compensate. Thus, proportionally more energy is allocated to storage at the expense of growth in the more stressful environment.

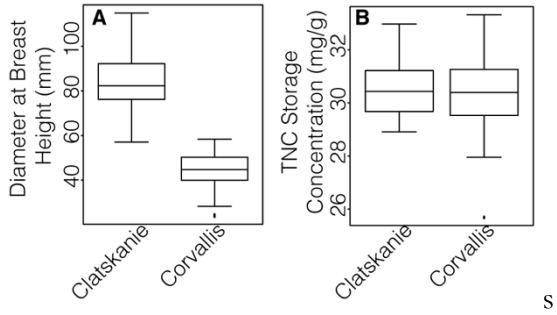

s

Figure 5. (A) Genetic variation in diameter at breast height (DBH) as compared to (B) genetic variation in total nonstructural carbohydrates as measured at each common garden.

Genotype-by-environment (GxE) plasticity in total stores, but not in proportion of stores in starch

Genetic variation in environmental response could provide a key mechanism through which populations can evolve a more adaptive response to future environmental stress. Here, we found that plastic variation in total storage is almost entirely comprised of genotype-by-environment interactions. The average total NSC storage concentrations between the two gardens only differ by 0.5 mg•g-1, but individual genotypes differ by -3.4 to 3.3 mg•g-1 between the two gardens. This flexibility amongst genotypes may be the result of intrinsic differences in response to environment [65] or slight variation in other traits correlated with storage. For example, if growing season length also exhibits some GxE, then individuals with slightly longer growing seasons may have more NSC to

allocate to storage than those with shorter seasons. Future research should investigate whether the observed genotype-by-environment variation represents local adaptation for plastic responses to the environment.

In contrast, plastic variation in the proportion of NSC stores in starch is almost entirely attributed to differences in environment and not GxE interactions. This finding further supports a model where by the amount of NSC residing in starch is driven by intrinsic enzymatic environmental limits. While GxE for this trait is lower than the amount of GxE for total NSC stores, there is a clear latitudinal pattern in the proportion of starch GxE variation (Figure S3). The trending correlation between latitude and the proportion of starch RDPI suggests that some genotypes may be more plastic than others in their ability to move between sugar and starch (Figure 5). In particular, genotypes from northern populations appear to have more flexibility between the two gardens. Put another way, northern genotypes are more responsive to environmental differences between the two sites. One possible explanation for this trend is that their starch degradation enzymes may be more sensitive to temperature fluctuations or are able to continue to act at slightly lower temperatures than those from southern populations. This may be beneficial to trees in northern latitudes experiencing extreme temperature lows and large temperature swings throughout the day. Although the amount of variation explained by GxE interactions may be small, the importance for immediate environmental response may be very important and is worth further investigation.

Conclusion

Our study is the first of its kind to study heritable variation and plasticity in branch nonstructural carbohydrate storage. NSC stores have been demonstrated over the past decade to confer resilience to climate stress in woody species and are likely critical for plant response to future climate. We found high amounts of heritable variation in both the total NSC concentration of stores and the

proportion of stores that are found in starch versus sugar, indicating a range-wide potential for tree species to adaptively evolve. Furthermore, we found environmental plasticity in the amount of total NSC stores put into starch, a critical trait for responding to temperature extremes, and a potential plastic tradeoff between NSC storage and growth. Finally, we found consistent environmental plasticity across all genotypes in the proportion of NSCs stored as starch vs. sugar. Overall, we demonstrate that the concentration of total NSCs that trees store as well as the degree to which they partition these stores between soluble sugars and starch have both adaptive genetic variation and plasticity, potentially bolstering forest tree species against climate change in the short-and-long term.

Conclusion

In Chapter 1, I uncovered locally adapted, heritable variation in the storage of nonstructural carbohydrates for the first time and identified genomic loci significantly associated with the trait, indicating the potential for future adaptation in this trait. This variation follows a latitudinal cline, where trees from hotter/drier environments store higher concentrations of NSCs on average than trees from the colder/wetter northern sites. This heritable variation in NSC concentrations also positively correlates with heritable variation in growth rates and defense ability. Thus, at first glance, it appeared that investing in NSC storage did not lead a predicted tradeoff with other carbon sinks such as growth and defense. Trees that were good at one thing were good at all things.

However, when we accounted for differences in carbon supply, the story became more complex in Chapter 2. Trees from southern environments are taller and have longer growing seasons, enabling them to sequester more carbon in the common garden than their southern counterparts. Thus, when we relativized all sinks for carbon supply, true tradeoffs emerged. I uncovered a genetic tradeoff between growth rates and defense ability with NSC storage (ie. some trees store more and invest less in growth, and vice versa). Unlike in Chapter 1 however, this genetic tradeoff is not locally adapted, but found in all populations. Thus, there is ample standing variation across all populations for future selection to act upon should higher stores or higher growth be favored under future climates.

Finally, in Chapter 3 I measured plasticity in NSC storage. Trees are long-lived, immobile species that will need to adjust to our rapidly changing climate over shorter time-scales as well as long. I found that the degree to which NSCs are stored as sugars vs starch exhibited a lot of

environmental plasticity, where trees put more NSC into sugar when grown in a colder environment. Conversely, total storage concentrations exhibited little environmental plasticity, but genotypes varied widely in their responses (ie. High genotype-by-environment interaction). However, the heritable growth-storage tradeoff discovered in chapter 2 may also have plasticity. While total storage concentrations between the two common gardens remained the same on average, tree growth rates and phenological timing differed markedly, suggesting that one garden stored more and grew less, while the other grew more and stored less on average.

My results advance our basic understanding of the role of NSC stores in trees, how NSC stores vary with other carbon sinks, and the potential for NSC storage concentrations to evolve or acclimate in response to climate change. Further, the novel predictive framework I developed in Chapter 1 has the ability to both identify venerable populations to climate change and the alleles/genotypes necessary for genomic rescue and restoration. Taken all together, I advance both our knowledge base of NSC storage in trees and present new methodologies for predicting how trees will respond to future environmental change.

Appendix 1

Supplementary materials for Chapter 2

Table S1. Bud flush scoring rubric.

Bud Flush

Score	Phenological Stage
0	Buds tightly closed
1	Buds swollen/breaking/leaf primordia visible
2	Leaves emerging just outside the bud scales
3	Leaves fully emerged and unfolding
4	Leaves fully unfolded
5	Leaves fully expanded

Table S2. Bud set scoring rubric.

Bud Set Score	Phenological Stage
0	Actively Growing
1	Slowing down, some new leaves at apex
2	Single new leaf at apex, stipules forming
3	Stipules form a point at apex
4	Small reddish bud formed
5	Large reddish bud formed

Table S3. *Venturia* scoring rubric.

Venturia Score	Phenological Stage

0	No *Venturia* readily apparent
1	some leaves affected
2	more leaves affected, maybe a small number of petioles and terminal branch buds
3	many petioles and terminal buds affected, shepherds crook appearance common, still estimated to be less than one third of the canopy affected
4	many petioles and terminal buds affected, shepherds crook appearance common, estimated to be less than one third of the canopy affected

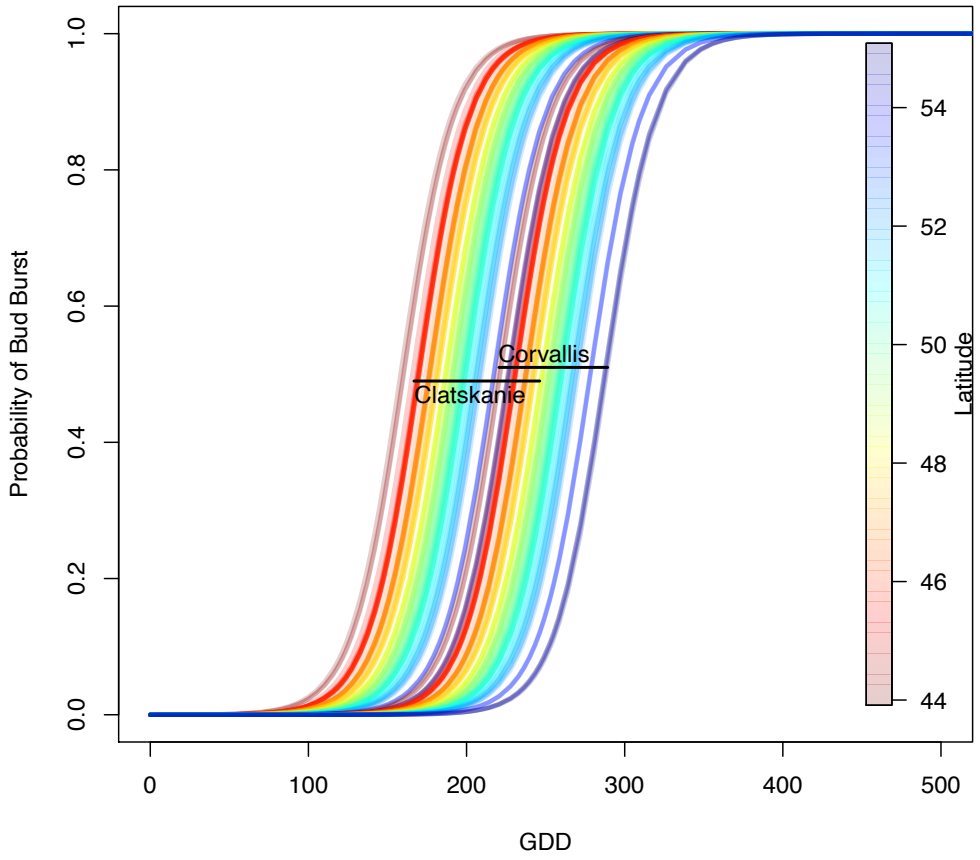

Figure 1. Probability of budburst based on latitude of genotype and growing degree days (GDD) accumulated in the garden.

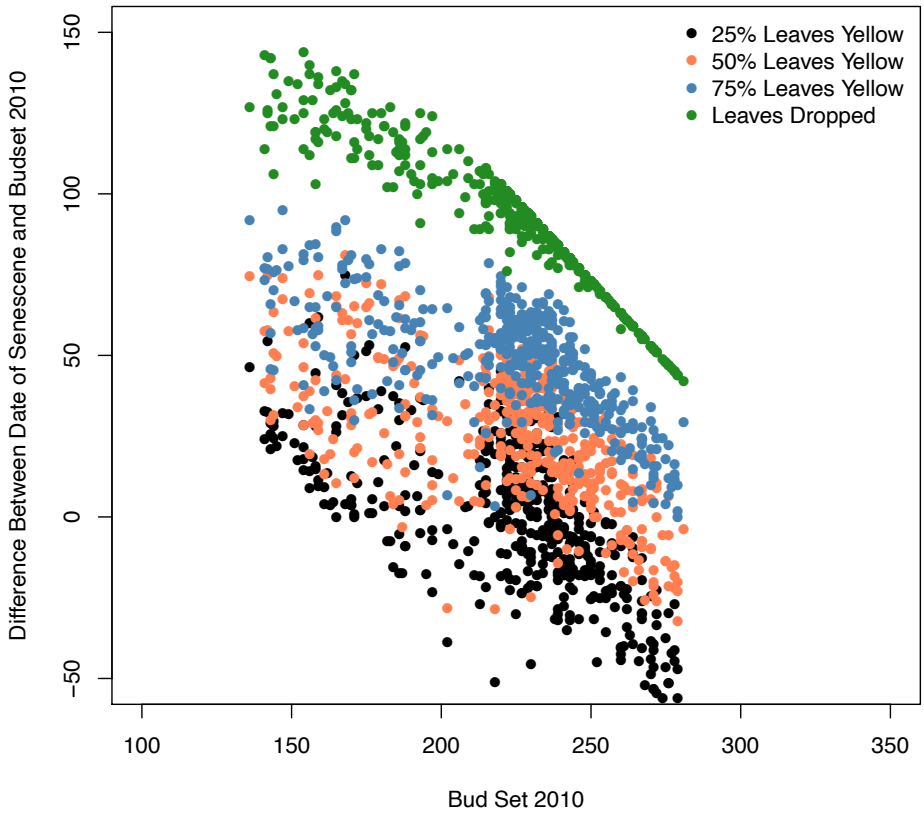

Figure S2. The relationship between days between bud set and senescence stage and date of budburst as measured in Vancouver, Canada between 2008-2010.

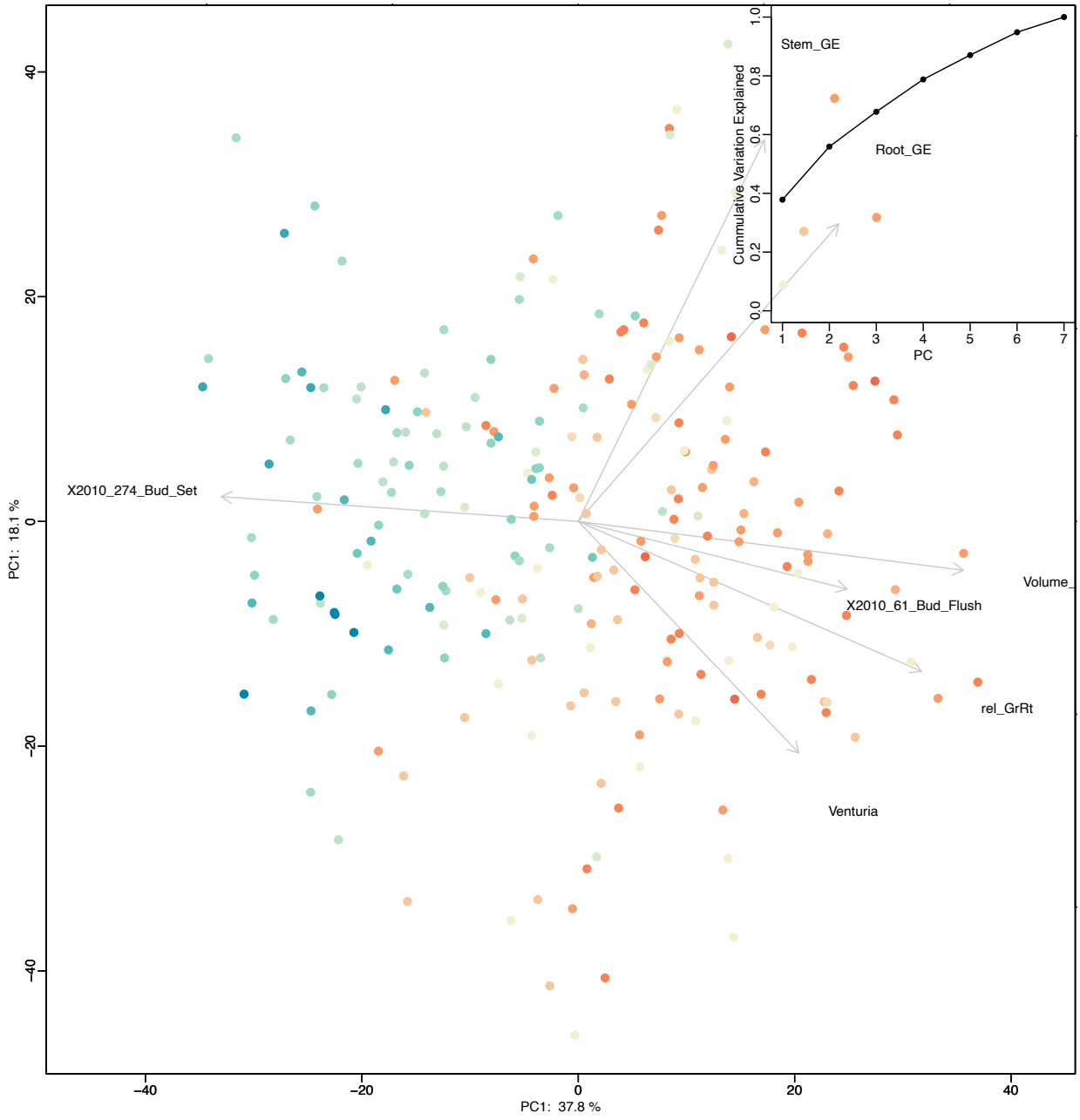

Figure S3. A replicate principle component analysis (PCA) and importance plot utilizing bud set and bud flush scores rather than calculated growing season length. Results demonstrate that using the calculated growing season length or raw scores does not alter trait relationships or results.

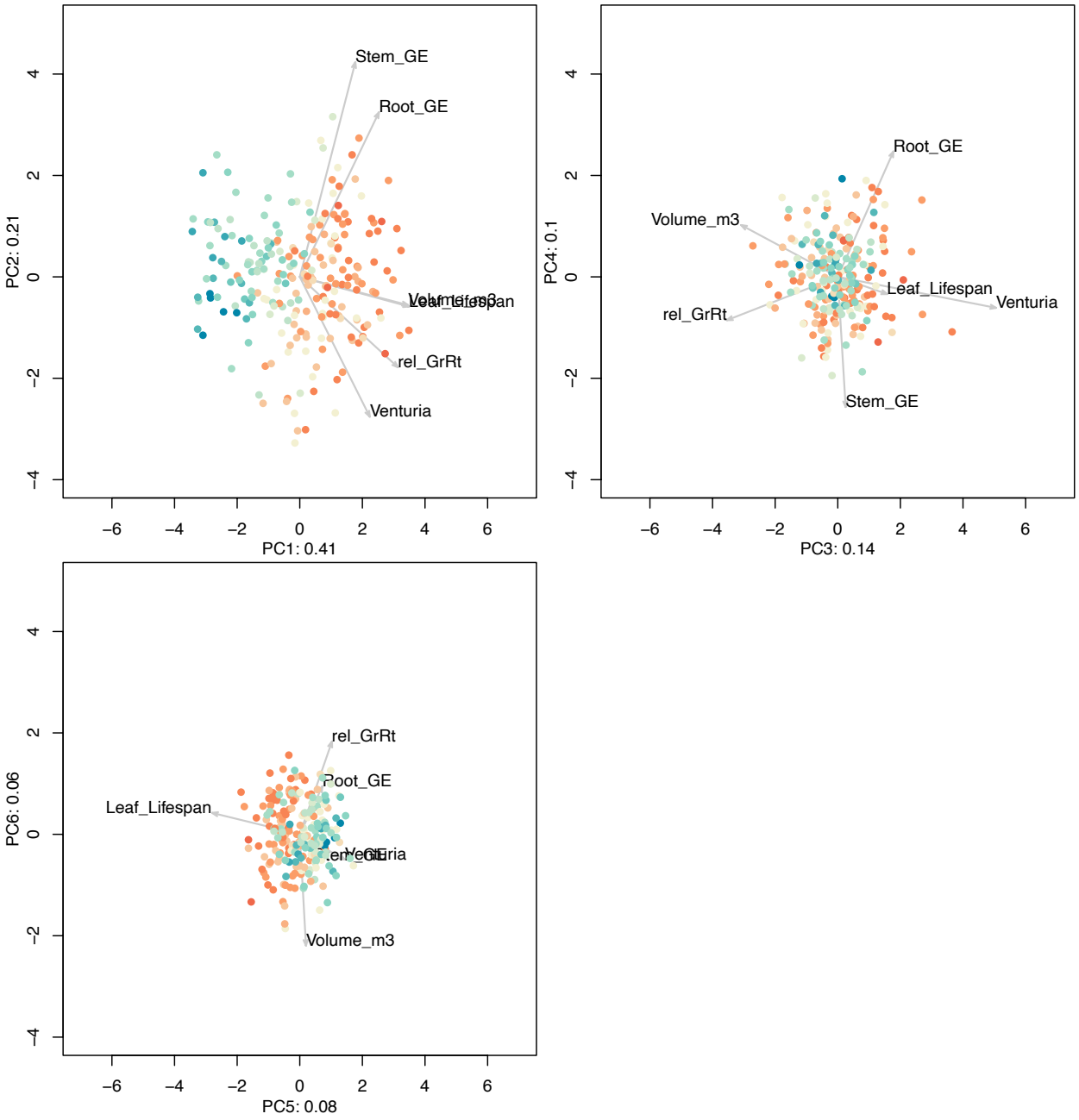

Figure S4. Results for all 6 PCs. Stem_GE and Root_GE are stem and root NSC concentrations, Volume_m3 is stem volume, Leaf Lifespan is growing season, *Venturia* is the inverse *Venturia* score, and rel_GrRt is relative growth rate of the diameter. Points represent genotypes and are colored by latitude of the genotypes provenance, where warmer colors are more southern clines.

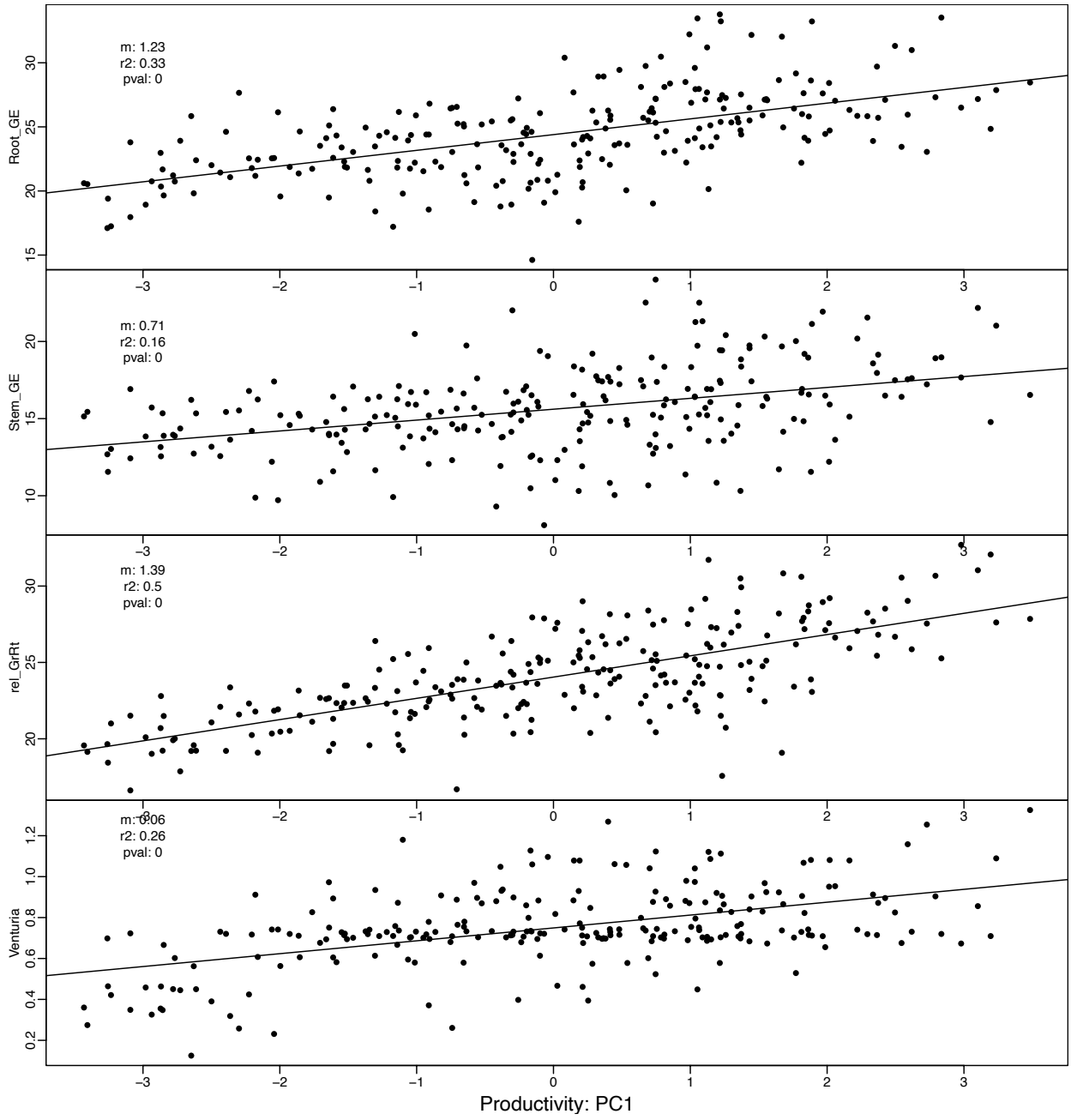

Figure S5. Carbon sinks plotted against "productivity", as measured by PC1 (Figure 4). Linear regression fits are shown, with slope, R^2 values, and p-value.

Appendix 2

Supplementary materials for Chapter 3

Table S1. Average and standard deviations of phenotypic values, as well as heritability and Q_{st} for bulk sugar (glucose+fructose+sucrose), starch, total nonstructural carbohydrates (TNC), and the proportion of starch to TNC. TNC values for stems and roots were previously reported.

Tissue	Trait	Mean	SD	H^2	Q_{st}
Stems	Sugar	13.4	5.3	0.46	0.34
	Starch	2.3	2.9	0.00	0.54
	TNC	15.6	6.0	0.43	0.31
	Proportion	0.1	0.2	0.01	0.66
Roots	Sugar	16.6	5.7	0.35	0.53
	Starch	7.5	6.8	0.21	0.03
	TNC	24.3	10.0	0.32	0.30
	Proportion	0.28	0.18	0.37	0.05

Table S2. Broad-sense heritability, Q_{st}, Relative Distance Plasticity Index (RDPI), and Plasticity (S) estimates of sugar and starch taken from branch wood samples. Also presented is the proportion of our plasticity estimate (S) that is attributable to genotype-by-environment interactions (GxE).

		H^2	Q_{st}	RDPI	S	(%) of S that is GxE
Branches	Sugar	0.21	0.05	0.08	0.58	22.0
	Starch	0.03	0.36	0.18	0.6	17.0

Table S3. Variance components from equations 1 and 4. All parameters were estimated using 6,000 random draws from the posterior distribution. Values calculated for sugar and starch concentrations of branch samples from black cottonwood trees grown in Clatskanie and Corvallis.

	Equation 1					Equation 4		
	(σ_{Gipg})	(σ_{Gpg})	(σ_{Gp})	(σ_G)	(β_G)	(σ_g)	(σ_G)	$(\sigma_{G:g})$
Sugar	21.589	5.303	0.535	246.471	0.9	2.1	4.8	2.5
Starch	4.652	0.068	0.076	16.56	-1.017	0.82	2.19	0.98

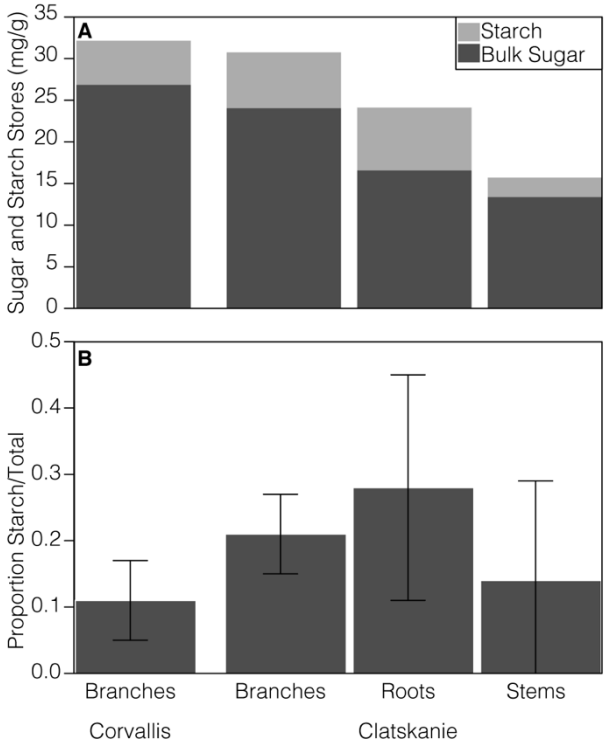

Figure S1. (A) Barplots of the amount of sugar and starch measured in each tissue in each garden as well as (B) the proportion of starch to the total amount of nonstructural carbohydrates (sugar + starch) measured. Error bars represent the standard deviation of each tissue respectively.

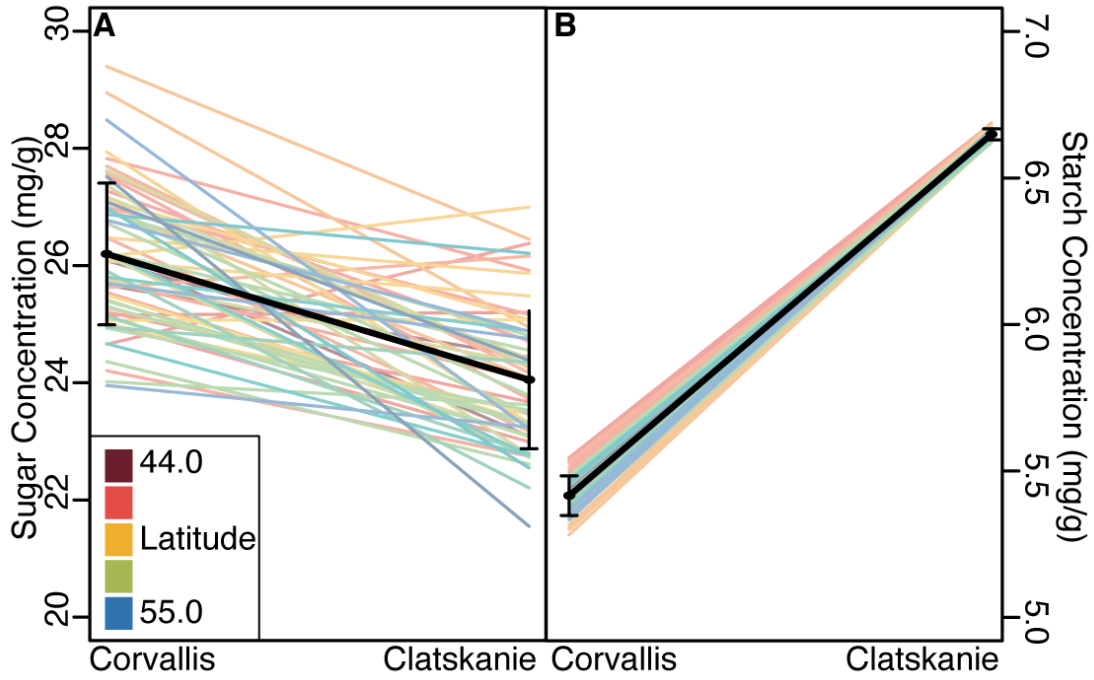

Figure S2. Plasticity between the two common gardens in (A) sugar concentration and (B) starch concentration. Black lines represent the average value across all genotypes, with error bars indicating

one standard deviation from the mean. The other lines are colored by latitude and each line represents a genotype, where genotype values were estimated using equation (1).

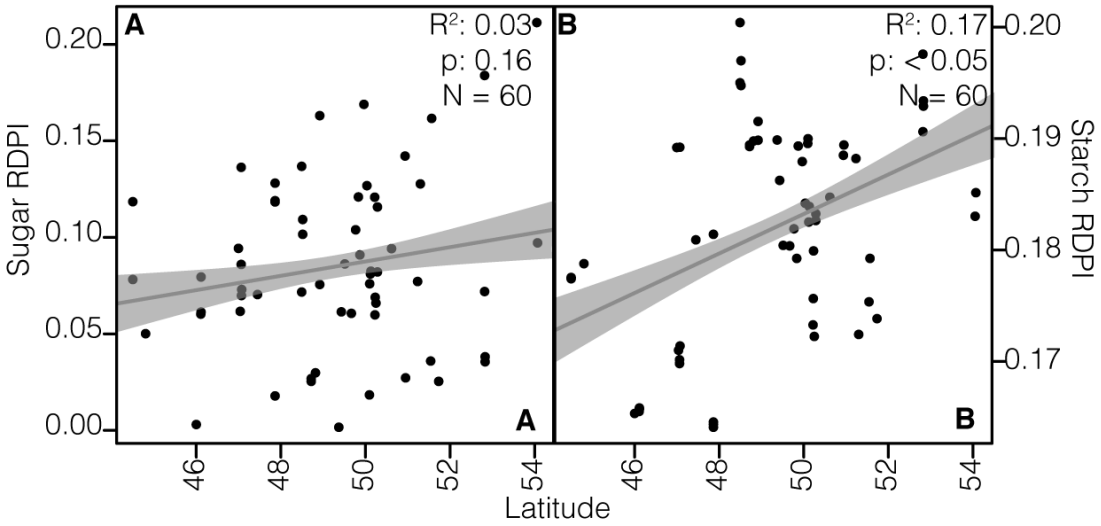

S3. The relative distance plasticity index (RDPI) of the amount of (A) sugar and (B) starch in branch woody tissue plotted by the latitude of each genotype's source location. Black dots represent each genotype's RDPI and the line fits are shaded gray for one standard deviation. A larger RDPI indicates that there is a larger percent change in genotypic trait values between gardens.

Works Cited

Works cited for chapters 2 & 3

1 FAO. Global Forest Resources Assessment 2005 – Progress towards sustainable forest management. (Rome, 2006).

2 Pan, Y. *et al.* A large and persistent carbon sink in the world's forests. *Science* **333**, 988-993, doi:10.1126/science.1201609 (2011).

3 Allen, C. D. *et al.* A global overview of drought and heat-induced tree mortality reveals emerging climate change risks for forests. *Forest Ecology and Management* **259**, 660-684, doi:10.1016/j.foreco.2009.09.001 (2010).

4 Raffa, K. *et al.* Cross-scale drivers of natural disturbances prone to anthropogenic amplification: the dynamics of bark beetle eruptions. *BioScience* **58**, 501-517 (2008).

5 IPCC. *Climate Change 2013: The Physical Science Basis. Contribution of Working Group I to the Fifth Assessment Report of the Intergovernmental Panel on Climate Change.* (Cambridge University Press, 2013).

6 Choat, B. Predicting thresholds of drought-induced mortality in woody plant species. *Tree Physiol* **33**, 669-671, doi:10.1093/treephys/tpt046 (2013).

7 Benito Garzón, M., Alía, R., Robson, T. M. & Zavala, M. A. Intra-specific variability and plasticity influence potential tree species distributions under climate change. *Global Ecology and Biogeography* **20**, 766-778, doi:10.1111/j.1466-8238.2010.00646.x (2011).

8 Iverson, L. R. & Prasad, A. M. Predicting abundance of 80 tree species following climate change in the Eastern United States. *Ecological Monographs* **68**, 465-485 (1998).

9 Hartmann, H. & Trumbore, S. Understanding the roles of nonstructural carbohydrates in forest trees - from what we can measure to what we want to know. *New Phytol* **211**, 386-403, doi:10.1111/nph.13955 (2016).

10 O'Brien, M. J., Leuzinger, S., Philipson, C. D., Tay, J. & Hector, A. Drought survival of tropical tree seedlings enhanced by non-structural carbohydrate levels. *Nature Climate Change* **4**, 710-714, doi:10.1038/nclimate2281 (2014).

11 Sala, A., Woodruff, D. R. & Meinzer, F. C. Carbon dynamics in trees: feast or famine? *Tree Physiol* **32**, 764-775, doi:10.1093/treephys/tpr143 (2012).

12 Wiley, E. *Towards a better understanding of nonstructural carbohydrate storage and carbon limitation in trees*, University of Pennsylvania, (2013).

13 Chapin III, S., Schulze, E.-D. & Mooney, H. A. The ecology and economics of storage in plants. *Annual Reviews* **21**, 423-447 (1990).

14 Plavcová, L. & Jansen, S. in *Functional and Ecological Xylem Anatomy* Ch. Chapter 8, 209-234 (2015).

15 Palacio, S., Gunter, H., Sala, A., Korner, C. & Millard, P. Does carbon storage limit tree growth? *New Phytologist* **201**, 1096-1100 (2014).

16 Furze, M. E. *et al.* Whole-tree nonstructural carbohydrate storage and seasonal dynamics in five temperate species. *New Phytol* **221**, 1466-1477, doi:10.1111/nph.15462 (2019).

17 Landhäusser, S. M. & Lieffers, V. J. Seasonal changes in carbohydrate reserves in mature northern Populus tremuloides clones. *Trees* **17**, 471-476, doi:10.1007/s00468-003-0263-1 (2003).

18 Plavcova, L., Hoch, G., Morris, H., Ghiasi, S. & Jansen, S. The amount of parenchyma and living fibers affects storage of nonstructural carbohydrates in young stems and roots of temperate trees. *Am J Bot* **103**, 603-612, doi:10.3732/ajb.1500489 (2016).

19 Richardson, A. D. *et al.* Seasonal dynamics and age of stemwood nonstructural carbohydrates in temperate forest trees. *New Phytol* **197**, 850-861, doi:10.1111/nph.12042 (2013).

20 Hoch, G., Richter, A. & Körner, C. Non-structural carbon compounds in temperate forest trees. *Plant, Cell and Environment* **26**, 1067-1081 (2003).

21 Richardson, A. D. *et al.* Distribution and mixing of old and new nonstructural carbon in two temperate trees. *New Phytol* **206**, 590-597, doi:10.1111/nph.13273 (2015).

22 Tuskan, G. A. *et al.* The Genome of Black Cottonwood, Populus trichocarpa (Torr. & Gray). *Science* **313** (2006).

23 McKown, A. D., Guy, R. D., Azam, M. S., Drewes, E. C. & Quamme, L. K. Seasonality and phenology alter functional leaf traits. *Oecologia* **172**, 653-665, doi:10.1007/s00442-012-2531-5 (2013).

24 McKown, A. D. *et al.* Geographical and environmental gradients shape phenotypic trait variation and genetic structure in Populus trichocarpa. *New Phytol* **201**, 1263-1276, doi:10.1111/nph.12601 (2014).

25 McKown, A. D. *et al.* Association genetics, geography and ecophysiology link stomatal patterning in Populus trichocarpa with carbon gain and disease resistance trade-offs. *Mol Ecol* **23**, 5771-5790, doi:10.1111/mec.12969 (2014).

26 McKown, A. D. *et al.* Genome-wide association implicates numerous genes underlying ecological trait variation in natural populations of Populus trichocarpa. *New Phytol* **203**, 535-553, doi:10.1111/nph.12815 (2014).

27 Burns, R. M. & Honkala, B. H. Silvics of North America: 1. Conifers; 2. Hardwoods. (U.S. Department of Agriculture Washington, DC, 1990).

28 Evans, L. M. *et al.* Population genomics of Populus trichocarpa identifies signatures of selection and adaptive trait associations. *Nat Genet* **46**, 1089-1096, doi:10.1038/ng.3075 (2014).

29 Yin, T. *et al.* Genome structure and emerging evidence of an incipient sex chromosome in Populus. *Genome Res* **18**, 422-430, doi:10.1101/gr.7076308 (2008).

30 Dietze, M. C. *et al.* Nonstructural carbon in woody plants. *Annu Rev Plant Biol* **65**, 667-687, doi:10.1146/annurev-arplant-050213-040054 (2014).

31 Michelot-Antalik, A., Granda, E., Fresneau, C. & Damesin, C. Evidence of a seasonal trade-off between growth and starch storage in declining beeches: assessment through stem radial increment, non-structural carbohydrates and intra-ring delta13C. *Tree Physiol* **39**, 831-844, doi:10.1093/treephys/tpz008 (2019).

32 Wiley, E. & Helliker, B. A re-evaluation of carbon stroage in trees lends greater support for carbon limitation to growth. *New Phytologist* **195**, 285-289 (2012).

33 Blumstein, M. *et al.* A new perspective on ecological prediction reveals limits to climate adaptation in a temperate tree species. *Current Biology* **30**, 1447-1453 (2020).

34 O'Brien, M. J., Reynolds, G., Ong, R. & Hector, A. Resistance of tropical seedlings to drought is mediated by neighbourhood diversity. *Nat Ecol Evol* **1**, 1643-1648, doi:10.1038/s41559-017-0326-0 (2017).

35 McDowell, N. & Sevanto, S. The mechanisms of carbons starvation: how, when, or does it even occur at all? *New Phytologist* **186**, 264-266 (2010).

36 Adams, H. D. *et al.* A multi-species synthesis of physiological mechanisms in drought-induced tree mortality. *Nat Ecol Evol* **1**, 1285-1291, doi:10.1038/s41559-017-0248-x (2017).

37 Sevanto, S., McDowell, N. G., Dickman, L. T., Pangle, R. & Pockman, W. T. How do trees die? A test of the hydraulic failure and carbon starvation hypotheses. *Plant Cell Environ* **37**, 153-161, doi:10.1111/pce.12141 (2014).

38 Bachofen, C. *et al.* No carbon "bet hedging" in pine seedlings under prolonged summer drought and elevated CO2. *Journal of Ecology* **106**, 31-46, doi:10.1111/1365-2745.12822 (2018).

39 Agrawal, A. A. A scale-dependent framework for trade-offs, syndromes, and specialization *Ecology* **101** (2020).

40 Agrawal, A. A., Conner, J. K. & Rasmann, S. Ch. 10, 243-268 (2010).

41 van Noordwijk, A. J. & de Jong, G. Acquisition and allocation of resources: their influence on variation in life history. *The American Naturalist* **128** (1986).

42 Linhart, Y. B. & Grant, M. C. Evolutionary significance of local genetic differentiation in plants. *Annual Review of Ecology, Evolution, and Systematics* **27**, 237-277 (1996).

43 Slavov, G. T. *et al.* Genome resequencing reveals multiscale geographic structure and extensive linkage disequilibrium in the forest tree Populus trichocarpa. *New Phytol* **196**, 713-725, doi:10.1111/j.1469-8137.2012.04258.x (2012).

44 de la Mata, R., Hood, S. & Sala, A. Insect outbreak shifts the direction of selection from fast to slow growth rates in the long-lived conifer Pinus ponderosa. *Proc Natl Acad Sci U S A* **114**, 7391-7396, doi:10.1073/pnas.1700032114 (2017).

45 Williams, J. W. & Jackson, S. T. Novel climates, no-analog communities, and ecological surprises. *Frontiers in Ecology and the Environment* **5**, 475-482, doi:10.1890/070037 (2007).

46 Davi, H., Barbaroux, C., Francois, C. & Dufrene, E. The fundamental role of reserves and hydraulic constraints in predicting LAI and carbon allocation in forests. *Agricultural and Forest Meteorology* **149**, 349-361, doi:10.1016/j.agrformet.2008.08.014 (2009).

47 Richardson, A. D. *et al.* Climate change, phenology, and phenological control of vegetation feedbacks to the climate system. *Agricultural and Forest Meteorology* **169**, 156-173, doi:10.1016/j.agrformet.2012.09.012 (2013).

48 Richardson, A. D. *et al.* Ecosystem warming extends vegetation activity but heightens vulnerability to cold temperatures. *Nature* **560**, 368-371, doi:10.1038/s41586-018-0399-1 (2018).

49 Soolanayakanahally, R. Y., Guy, R. D., Silim, S. N. & Song, M. Timing of photoperiodic competency causes phenological mismatch in balsam poplar (Populus balsamifera L.). *Plant Cell Environ* **36**, 116-127, doi:10.1111/j.1365-3040.2012.02560.x (2013).

50 Thornton, P. E. *et al.* (ed Oak Ridge National Lab DAAC) (Oak Ridge, TN, USA, 2018).

51 Holeski, L. M., Vogelzang, A., Stanosz, G. & Lindroth, R. L. Incidence of Venturia shoot blight in aspen (Populus tremuloides Michx.) varies with tree chemistry and genotype. *Biochemical Systematics and Ecology* **37**, 139-145, doi:10.1016/j.bse.2009.02.003 (2009).

52 Blumstein, M. *et al.* A new perspective on ecological prediction reveals limits to climate adaptation in a temperate tree species. *In Submission* (2019).

53 Chow, P. S. & Landhausser, S. M. A method for routine measurements of total sugar and starch content in woody plant tissues. *Tree Physiology* **24**, 1129-1136 (2004).

54 Landhausser, S. M. *et al.* Standardized protocols and procedures can precisely and accurately quantify non-structural carbohydrates. *Tree Physiol* **38**, 1764-1778, doi:10.1093/treephys/tpy118 (2018).

55 Josephs, E. B., Berg, J. J., Ross-Ibarra, J. & Coop, G. Detecting adaptive differentiation in structured populations with genomic data and common gardens. *Genetics* **211**, doi:10.1101/368506 (2019).

56 Whitlock, M. C. & Gilbert, K. J. Qst in a hierarchical structured population. *Molecular Ecology Resources* **12**, 481-483 (2012).

57 IPCC. in *Climate Change 2013: The Physical Science Basis. Contribution of Working Group I to the Fifth Assessment Report of the Intergovernmental Panel on Climate Change* (eds T.F. Stocker *et al.*) Ch. AI, 1311–1394 (Cambridge University Press, 2013).

58 McDowell, N. *et al.* Drivers and mechanisms of tree mortality in moist tropical forests. *New Phytol* **219**, 851-869, doi:10.1111/nph.15027 (2018).

59 Anderegg, W. R. *et al.* Tree mortality from drought, insects, and their interactions in a changing climate. *New Phytol* **208**, 674-683, doi:10.1111/nph.13477 (2015).

60 Anderegg, W. R. *et al.* Meta-analysis reveals that hydraulic traits explain cross-species patterns of drought-induced tree mortality across the globe. *Proc Natl Acad Sci U S A* **113**, 5024-5029, doi:10.1073/pnas.1525678113 (2016).

61 Pritzkow, C., Williamson, V., Szota, C., Trouve, R. & Arndt, S. K. Phenotypic plasticity and genetic adaptation of functional traits influences intra-specific variation in hydraulic efficiency and safety. *Tree Physiol* **40**, 215-229, doi:10.1093/treephys/tpz121 (2020).

62 Wortemann, R. *et al.* Genotypic variability and phenotypic plasticity of cavitation resistance in Fagus sylvatica L. across Europe. *Tree Physiol* **31**, 1175-1182, doi:10.1093/treephys/tpr101 (2011).

63 Valladares, F., Sanchez-Gomez, D. & Zavala, M. A. Quantitative estimation of phenotypic plasticity: bridging the gap between the evolutionary concept and its ecological applications. *Journal of Ecology* **94**, 1103-1116, doi:10.1111/j.1365-2745.2006.01176.x (2006).

64 Valladares, F. *et al.* The effects of phenotypic plasticity and local adaptation on forecasts of species range shifts under climate change. *Ecology Letters* **17**, 1351-1364, doi:10.1111/ele.12348 (2014).

65 Des Marais, D. L., Hernandez, K. M. & Juenger, T. E. Genotype-by-Environment Interaction and Plasticity: Exploring Genomic Responses of Plants to the Abiotic Environment. *Annual Review of Ecology, Evolution, and Systematics* **44**, 5-29, doi:10.1146/annurev-ecolsys-110512-135806 (2013).

66 Anderson, J. T., Inouye, D. W., McKinney, A. M., Colautti, R. I. & Mitchell-Olds, T. Phenotypic plasticity and adaptive evolution contribute to advancing flowering phenology in response to climate change. *Proc Biol Sci* **279**, 3843-3852, doi:10.1098/rspb.2012.1051 (2012).

67 Aitken, S. N., Yeaman, S., Holliday, J. A., Wang, T. & Curtis-McLane, S. Adaptation, migration or extirpation: climate change outcomes for tree populations. *Evol Appl* **1**, 95-111, doi:10.1111/j.1752-4571.2007.00013.x (2008).

68 Davis, M. B., Shaw, R. G. & Etterson, J. R. Evolutionary responses to changing climate. *Ecology* **86**, 1704-1714 (2005).

69 McDowell, N. *et al.* Mechanisms of plant survival and mortality during drought: why do some plants survive while others succumb to drought? *New Phytol* **178**, 719-739, doi:10.1111/j.1469-8137.2008.02436.x (2008).

70 Martínez-Vilalta, J. *et al.* Dynamics of non-structural carbohydrates in terrestrial plants: a global synthesis. *Ecological Monographs* **86**, 495-516, doi:10.1002/ecm.1231 (2016).

71 Kaplan, F. & Guy, C. L. beta-Amylase induction and the protective role of maltose during temperature shock. *Plant Physiol* **135**, 1674-1684, doi:10.1104/pp.104.040808 (2004).

72 Krasensky, J. & Jonak, C. Drought, salt, and temperature stress-induced metabolic rearrangements and regulatory networks. *J Exp Bot* **63**, 1593-1608, doi:10.1093/jxb/err460 (2012).

73 Thalmann, M. & Santelia, D. Starch as a determinant of plant fitness under abiotic stress. *New Phytol* **214**, 943-951, doi:10.1111/nph.14491 (2017).

74 Tixier, A., Orozco, J., Roxas, A. A., Earles, J. M. & Zwieniecki, M. A. Diurnal Variation in Nonstructural Carbohydrate Storage in Trees: Remobilization and Vertical Mixing. *Plant Physiol* **178**, 1602-1613, doi:10.1104/pp.18.00923 (2018).

75 Wurth, M. K., Pelaez-Riedl, S., Wright, S. J. & Korner, C. Non-structural carbohydrate pools in a tropical forest. *Oecologia* **143**, 11-24, doi:10.1007/s00442-004-1773-2 (2005).

76 Mitchell, P. J. *et al.* Drought response strategies define the relative contributions of hydraulic dysfunction and carbohydrate depletion during tree mortality. *New Phytol* **197**, 862-872, doi:10.1111/nph.12064 (2013).

77 Landhäusser, S. M. & Lieffers, V. J. Defoliation increases risk of carbon starvation in root systems of mature aspen. *Trees* **26**, 653-661, doi:10.1007/s00468-011-0633-z (2011).

78 Kempa, S., Krasensky, J., Dal Santo, S., Kopka, J. & Jonak, C. A central role of abscisic acid in stress-regulated carbohydrate metabolism. *PLoS One* **3**, e3935, doi:10.1371/journal.pone.0003935 (2008).

79 Kanai, M. *et al.* Common reed produces starch granules at the shoot base in response to salt stress. *New Phytol* **176**, 572-580, doi:10.1111/j.1469-8137.2007.02188.x (2007).

80 Ma, T. *et al.* Genomic insights into salt adaptation in a desert poplar. *Nat Commun* **4**, 2797, doi:10.1038/ncomms3797 (2013).

81 Goyal, A. Osmoregulation in Dunaliella, Part II: Photosynthesis and starch contribute carbon for glycerol synthesis during a salt stress in Dunaliella tertiolecta. *Plant Physiol Biochem* **45**, 705-710, doi:10.1016/j.plaphy.2007.05.009 (2007).

82 Chen, H.-J., Chen, J.-Y. & Wang, S.-J. Molecular regulation of starch accumulation in rice seedling leaves in response to salt stress. *Acta Physiologiae Plantarum* **30**, 135-142, doi:10.1007/s11738-007-0101-y (2007).

83 Vasseur, F., Pantin, F. & Vile, D. Changes in light intensity reveal a major role for carbon balance in Arabidopsis responses to high temperature. *Plant Cell Environ* **34**, 1563-1576, doi:10.1111/j.1365-3040.2011.02353.x (2011).

84 Nagao, M., Minami, A., Arakawa, K., Fujikawa, S. & Takezawa, D. Rapid degradation of starch in chloroplasts and concomitant accumulation of soluble sugars associated with ABA-induced freezing tolerance in the moss Physcomitrella patens. *J Plant Physiol* **162**, 169-180, doi:10.1016/j.jplph.2004.06.012 (2005).

85 Kaplan, F. & Guy, C. L. RNA interference of Arabidopsis beta-amylase8 prevents maltose accumulation upon cold shock and increases sensitivity of PSII photochemical efficiency to freezing stress. *Plant J* **44**, 730-743, doi:10.1111/j.1365-313X.2005.02565.x (2005).

86 Hoermiller, II *et al.* Subcellular reprogramming of metabolism during cold acclimation in Arabidopsis thaliana. *Plant Cell Environ* **40**, 602-610, doi:10.1111/pce.12836 (2017).

87 Nuismer, S. L. & Gandon, S. Moving beyond common-garden and transplant designs: insight into the causes of local adaptation in species interactions. *Am Nat* **171**, 658-668, doi:10.1086/587077 (2008).

88 Oleksyn, J., Zytkowiak, R., Karolewski, P., Reich, P. B. & Tjoelker, M. G. Genetic and environmental control of seasonal carbohydrate dynamics in tress of diverse Pinus sylvestris populations. *Tree Physiology* **20**, 837-847 (1999).

89 R: A Language and Environment for Statistical Computing (Vienna, Austria, 2018).

90 Hufkens, K., Basler, J. D., Milliman, T., Melaas, E. & Richardson, A. D. An interated phenology modelling framework in R: Phenology modelling with phenor. *Methods in Ecology and Evolution* **9**, 1-10 (2018).

91 Oksanen, J. *et al. vegan: Community Ecology Package*, <https://CRAN.R-project.org/package=vegan> (2018).

92 Stopher, K. V. *et al.* Shared spatial effects on quantitative genetic parameters: accounting for spatial autocorrelation and home range overlap reduces estimates of heritability in wild red deer. *Evolution* **66**, 2411-2426, doi:10.1111/j.1558-5646.2012.01620.x (2012).

93 fields: Tools for spatial data (University Corporation for Atmospheric Research, Boulder, CO, USA, 2017).

94 RStan Getting Started (2014).

95 Spitze, K. Population structure in *Daphnia obtusa*: quantitative genetic and allozymic variation. . *Genetics* **135**, 367-374 (1993).

96 Whitlock, M. C. & Gilbert, K. J. Q(ST) in a hierarchically structured population. *Molecular Ecology Resources* **12**, 481-483, doi:10.1111/j.1755-0998.2012.03122.x (2012).

97 Scheiner, S. M. & Goodnight, C. J. The comparison of phenotypic plasticity and genetic variation in populations of the grass Danthonia spicata. *Evolution* **38** (1984).

98 Goodrich, B., Gabry, J., Ali, I. & Brilleman, S. rstanarm: Bayesian applied regression modelin via Stan. (2019).

99 Scheiner, S. M. & Lyman, R. F. The genetics of phenotypic plasticity. *Journal of Evolutionary Biology* **2**, 95-107 (1989).

100 Pollock, C. J. & Lloyd, E. J. The effect of low temperatures upon starch, sucrose, and fructan synthesis in leaves. *Annals of Botany* **60**, 231-235 (1987).

101 Hartmann, H. *et al.* Identifying differences in carbohydrate dynamics of seedlings and mature trees to improve carbon allocation in models for trees and forests. *Environmental and Experimental Botany* **152**, 7-18, doi:10.1016/j.envexpbot.2018.03.011 (2018).

102 Adams, H. D. *et al.* Nonstructural leaf carbohydrate dynamics of Pinus edulis during drought-induced tree mortality reveal role for carbon metabolism in mortality mechanism. *New Phytol* **197**, 1142-1151, doi:10.1111/nph.12102 (2013).

103 Hartmann, H., Ziegler, W., Trumbore, S. & Knapp, A. Lethal drought leads to reduction in nonstructural carbohydrates in Norway spruce tree roots but not in the canopy. *Functional Ecology* **27**, 413-427, doi:10.1111/1365-2435.12046 (2013).

104 Zwieniecki, M. A., Tixier, A. & Sperling, O. Temperature-assisted redistribution of carbohydrates in trees. *Am J Bot* **102**, 1216-1218, doi:10.3732/ajb.1500218 (2015).

105 Tixier, A., Gambetta, G. A., Godfrey, J., Orozco, J. & Zwieniecki, M. A. Non-structural Carbohydrates in Dormant Woody Perennials; The Tale of Winter Survival and Spring Arrival. *Frontiers in Forests and Global Change* **2**, doi:10.3389/ffgc.2019.00018 (2019).

106 Gibon, Y. *et al.* Adjustment of growth, starch turnover, protein content and central metabolism to a decrease of the carbon supply when Arabidopsis is grown in very short photoperiods. *Plant Cell Environ* **32**, 859-874, doi:10.1111/j.1365-3040.2009.01965.x (2009).

107 Sperling, O., Silva, L. C. R., Tixier, A., Theroux-Rancourt, G. & Zwieniecki, M. A. Temperature gradients assist carbohydrate allocation within trees. *Sci Rep* **7**, 3265, doi:10.1038/s41598-017-03608-w (2017).

108 Alberto, F. *et al.* Adaptive responses for seed and leaf phenology in natural populations of sessile oak along an altitudinal gradient. *J Evol Biol* **24**, 1442-1454, doi:10.1111/j.1420-9101.2011.02277.x (2011).

109 Hall, D. *et al.* Adaptive population differentiation in phenology across a latitudinal gradient in European aspen (Populus tremula, L.): a comparison of neutral markers, candidate genes and phenotypic traits. *Evolution* **61**, 2849-2860, doi:10.1111/j.1558-5646.2007.00230.x (2007).

110 Keller, S. R. *et al.* Climate-driven local adaptation of ecophysiology and phenology in balsam poplar, Populus balsamifera L. (Salicaceae). *Am J Bot* **98**, 99-108, doi:10.3732/ajb.1000317 (2011).

111 Smith, A. M. & Stitt, M. Coordination of carbon supply and plant growth. *Plant Cell Environ* **30**, 1126-1149, doi:10.1111/j.1365-3040.2007.01708.x (2007).